OULU UNIVERSITY OF
APPLIED SCIENCES

Jukka Lämsä

AUTOMATION OF MEASUREMENTS FOR A RADIO FREQUENCY TRANSMITTER AND RECEIVER

AUTOMATION OF MEASUREMENTS FOR A RADIO FREQUENCY TRANSMITTER AND RECEIVER

Jukka Lämsä
Bachelor's thesis
Spring 2014
Degree Programme in Information Technology and Telecommunications
Oulu University of Applied Sciences

TIIVISTELMÄ

Oulun ammattikorkeakoulu
Tietotekniikan koulutusohjelma, langattomien laitteiden suuntautumisvaihtoehto

Tekijä: Jukka Lämsä
Opinnäytetyön nimi: Automation of measurements for a radio frequency transmitter and receiver
Työn ohjaajat: Timo Vainio, Marko Leinonen
Valmistumislukukausi ja -vuosi: Kevät 2014 Sivumäärä: 102 + 2 liitettä

Opinnäytetyön tavoitteena oli automatisoida radiolähetinvastaanottimissa käytettyjen komponenttien suorituskykymittaukset ja niihin kuuluva tulosten keruu. Päätavoite oli kehittää National Instruments LabVIEW- ohjelmointikielellä mittausautomaatiorutiinit viidelle eri perusmittaukselle.

Jotta automatisointi voitiin toteuttaa ja tavoite saavuttaa, taustatutkimusta täytyi tehdä sekä radiotekniikkaan että mittausjärjestelmiin ja niiden ohjaukseen. Lisäksi toteutetun ohjelmiston täytyi olla modulaarinen, jotta sen osasia voidaan jatkokäyttää erilaisissa tarkoituksissa.

Työ suoritettiin OY LM Ericsson AB:n Oulussa sijaitsevalle toimipisteelle, joka on keskittynyt kehittämään tukiasemia piensolukäyttöön. Tuloksena työstä saatiin työn suunnittelussa määritellyt viisi mittausta suorittavat automaatiorutiinit, sekä lisäksi useita pienempiä automatisoituja mittausrutiineja jotka ovat sellaisenaan jatkosovelluksia silmällä pitäen käyttökelpoisia. Automatisoitujen mittausten tuloksien todettiin olevan vertailukelpoisia käsin tehtyihin.

Johtopäätöksenä työn todettiin olevan onnistunut sillä mittausten automatisoinnilla säästettiin valtavasti aikaa komponenttien suorituskykyä tutkittaessa. Lisäksi ohjelmistomoduleilla kyetiin suorittamaan lisämittauksia, kuten esimerkiksi signaalinkäsittelyalgoritmien testausta.

Asiasanat:
Radiotekniikka, automaatio, mittaustekniikka, mittauslaitteet, signaalianalyysi

ABSTRACT

Oulu University of Applied Sciences
Degree Programme in Information Technology and Telecommunications, Option of Wireless Devices

Author: Jukka Lämsä
Title of thesis: Automation of Measurements for a Radio Frequency Transmitter and Receiver
Supervisors: Timo Vainio, Marko Leinonen
Term and year of completion: Spring 2014 Pages: 102 + 2 appendices

The objective of this Bachelor's thesis was to automate performance measurements done in the development of a radio transmitter and a receiver. The main objective was to develop measurement automation routines for five basic performance measurements using National Instruments LabVIEW as a software development environment.

In order to meet this objective, a study of radio technology and their architecture was required. Additionally, a study of measurement systems and control was required. The developed software had to be modular to ease further development in future.

The thesis was done for OY LM Ericsson AB site in Oulu, which is concentrated on the development of small-cell base station products. Measurement results gained with automation software were compared to those of manual measurements. As a result, main five measurements were successfully automated, and the results obtained matched those of manual measurements in terms of accuracy. Also, multiple smaller measurement automation routines were developed to ease automation development in the future.

The thesis work was evaluated successful because of time and resources saved by the automation. In addition, it was possible to use the software modules in different additional measurements, for example in the testing of signal processing algorithms.

Keywords:
Radio frequency, performance evaluation, RF signals, instrumentation

PREFACE

This Bachelor's thesis is done for OY LM Ericsson AB Oulu site during the autumn of 2013 and spring of 2014.

I want to thank all my colleagues in OY LM Ericsson AB Oulu for this opportunity to work with you. Special thanks go to my supervisor Marko Leinonen for all the support, feedback and encouragement during the thesis work.

Additionally, I want to thank my girlfriend and my family for all the support during my studies and the thesis work.

Last but not least, special thanks go to my classmates for all the support and help during these years.

March 2014, Oulu.

Jukka Lämsä

CONTENTS

1 INTRODUCTION 13
2 RF TRANSMITTER AND RECEIVER 15
2.1 RF transmitter components 16
2.1.1 Modulator 16
2.1.2 Digital-to-analog converter 18
2.1.3 Mixer 20
2.1.4 Variable gain amplifier and power amplifier 21
2.1.5 Duplex filter 22
2.2 RF receiver components 24
2.2.1 Duplex filter 25
2.2.2 LNA 25
2.2.3 Quadrature demodulator 25
2.2.3.1 Mixer 27
2.2.3.2 Low-pass/IF filter 28
2.2.4 VGA 28
2.2.5 Analog-to-digital converter 28
3 RF TRANSCEIVER MEASUREMENTS 30
3.1 Linearity of the active transmitter components 31
3.2 Power added efficiency 41
3.3 Receiver sensitivity 43
3.4 Receiver adjacent channel selectivity 45
3.5 Linearity of passive components 47
4 OVERVIEW OF A MEASUREMENT AND AUTOMATION ENVIRONMENT 50
4.1 About LabVIEW 50
4.2 Overview of an example measurement system 54
4.3 Instrument control methods 57
4.3.1 GPIB interface 57
4.3.2 VISA software control interface 59
4.3.3 Instrument control problems during development 61
4.4 Software integrations and interfaces 62

4.4.1 Software integration example 63
4.4.2 Problems related in software integration 63
5 AUTOMATION SOFTWARE FOR PASSIVE INTERMODULATION MEASUREMENTS 65
5.1 Measurement system 65
5.2 User interface of passive intermodulation measurement software 67
5.3 Block diagrams and functional description 68
5.3.1 Calibration software 68
5.3.2 Instrument control 70
5.3.2.1 Signal generator control VI 71
5.3.2.2 Spectrum analyser VIs 73
5.3.2.3 Network analyser VI 75
5.3.3 Data logging 76
5.4 Example results 79
5.5 Problems during development 80
5.6 Conclusions 80
6 AUTOMATION SOFTWARE FOR POWER AMPLIFIER MEASUREMENTS 81
6.1 Measurement system 82
6.2 User interface of power amplifier measurement automation software 83
6.3 Block diagram and a functional description 84
6.3.1 Environment setting 85
6.3.2 ACP measurement 86
6.3.3 PAE measurement 87
6.3.4 Data logging 92
6.4 Problems during development 94
6.5 Conclusions 95
7 SUMMARY AND CONCLUSIONS 96

ABBREVIATIONS

3GPP	3rd generation partnership project
ACP	Adjacent channel power
ACLR	Adjacent channel leakage ratio
ADC	Analog to digital converter
ASK	Amplitude shift keying
BTS	Base transceiver station
COM	Communication port
CSV	Comma separated value
CW	Continuous wave
DAC	Digital to analog converter
dB	Decibel
DC	Direct current
EMC	Electromagnetic compatibility
FDD	Frequency division duplexing
GPIB	General purpose interface bus
IF	Intermediate frequency
IM	Intermodulation
IMD	Intermodulation distortion
LAN	Local area network
LNA	Low noise amplifier

LPF	Low pass filter
LTE	Long term evolution
LXI	LAN-based extensions for instrumentation
PA	Power amplifier
PAE	Power added efficiency
PCB	Printed circuit board
PIM	Passive intermodulation
QAM	Quadrature amplitude modulation
RF	Radio frequency
RX	Receiver/receive
TDD	Time division duplexing
TX	Transmitter/transmit
UE	User equipment
WCDMA	Wideband code domain multiple access
VGA	Variable gain amplifier
VI	Virtual instrument
VISA	Virtual instrument software architecture

LIST OF PICTURES

Picture 1. Screenshot of an adjacent channel power measurement (17) 38
Picture 2. Example case (17) 45

Picture 3. Example of relations between a front panel and a block diagram (17) 50
Picture 4. LabVIEW front panel example with controls and indicators (17) 51
Picture 5. Block diagram linked to a front panel example in picture 5 (17) 51
Picture 6. Example front panel with multiplication and ASCII string concatenation operations done in a block diagram (17) 52
Picture 7. Block diagram with multiplication and string concatenation operations, linked to the front panel example in picture 6 (17) 52
Picture 8. Example of linking controls and indicators into the VI I/O terminals (17) 53
Picture 9. Block diagram of the sub-VI example in picture 8 (17) 53
Picture 10. Example of a sub-VI usage. (17) 54
Picture 11. VISA resource name control in LabVIEW with a drop-down menu opened (17) 60
Picture 12. Example of a simple VISA query (17) 60
Picture 13. User interface of a passive intermodulation measurement and analysis VI 67
Picture 14. Block diagram of the calibration phase of a passive intermodulation measurement VI 69
Picture 15. One of dialog boxes guiding the user during a calibration routine .. 69
Picture 16. Block diagram of the measurement phase of the passive intermodulation measurement VI 70
Picture 17. Front panel of the signal generator control VI 71
Picture 18. Block diagram of the signal generator control VI 71
Picture 19. Decimal separator setting, a number to a string conversion and concatenation operations 72
Picture 20. The select operations 73
Picture 21. Front panel and a block diagram of a reference level setting VI 73
Picture 22. Front panel of a CW power measurement VI 74
Picture 23. Block diagram of a CW power measurement VI 74
Picture 24. Block diagram of the VI performing an auto scaling function and an OPC query 75
Picture 25. Front panel of the network analyzer VI 76

Picture 26. An example .CSV-file opened in a text editor 77
Picture 27. Example .CSV-file in Excel 77
Picture 28. Front panel of the data logging VI 78
Picture 29. Block diagram of the data logging VI. In section 1, the file operations are seen. In section 2, the numerical array is parsed into a string in a .CSV format 78
Picture 30. Illustration of the measurement system used (5) 82
Picture 31.Block diagram of the TX measurement automation software 83
Picture 32. User interface of the TX measurement automation software 83
Picture 33. Block diagram of the main VI of the TX measurement automation 84
Picture 34. Front panel of the environmental chamber control VI 85
Picture 35. Front panel of the ACP measurement VI 86
Picture 36. Block diagram of the ACP measurement VI 86
Picture 37. Block diagram the ACP result query VI 87
Picture 38. Front panel of the PAE measurement VI 88
Picture 39. Block diagram of the PAE measurement VI 89
Picture 40. Front panel of the Multimeter VI 89
Picture 41. Block diagram of the multimeter VI 90
Picture 42. Front panel of the power meter VI 90
Picture 43. Block diagram of the power meter VI 91
Picture 44. Front panel of the PAE calculation VI 91
Picture 45. Block diagram of the PAE calculation VI 92
Picture 46. Front panel of the screenshot capturing and transferring VI 92
Picture 47. Block diagram of the screenshot capturing and transferring VI 93
Picture 48. Front panel of the screenshot capturing VI 93
Picture 49. Block diagram of the screenshot capture VI 94

LIST OF FIGURES

Figure 1. Block diagram of an example RF transmitter architecture (17) 16
Figure 2. Example of a QAM constellation diagram (22) 17
Figure 3. Block diagram of a QAM modulator (17) 17
Figure 4. DAC output before a reconstruction filter (17) 19

Figure 5. DAC output after a reconstruction filter (17) 20
Figure 6. Simplified PLL architecture (17) 21
Figure 7. RX side frequency response of an example duplexer (32) 22
Figure 8. TX side frequency response of an example duplexer (32) 23
Figure 9. Block diagram of an example RF receiver architecture (17) 24
Figure 10. Block diagram of the quadrature demodulator used in the example receiver architecture (17) 24
Figure 11. Block diagram of a QAM demodulator (17) 25
Figure 12. Illustration of ADC sampling of an analog signal (17) 28
Figure 13. MATLAB power spectrum estimate of a wideband signal fed into generic nonlinear model (17) 34
Figure 14. MATLAB plot of an original two-tone input signal (17) 35
Figure 15. MATLAB plot of a 3rd degree model result (17) 35
Figure 16. MATLAB plot of a 5th degree model result (17) 36
Figure 17. IMD3 frequencies (4). 37
Figure 18. Example of amplifier measurement results, measured from a standard instrumentation amplifier (17) 39
Figure 19. Example of a power added efficiency measurement result, measured from a standard instrumentation amplifier (17) 43
Figure 20. Example measurement system (17) 55
Figure 21. Star cabling topology defined in standard (17) 58
Figure 22. Linear, "daisy chain" GPIB topology used in a developed measurement automation (17) 58
Figure 23. Illustration of a VISA interface data flow (17) 59
Figure 24. Example of a feedback loop used in a measurement automation (17) 61
Figure 25. Example of software integration interfaces (17) 62
Figure 26. Illustration of the measurement system used for a passive intermodulation measurement (17) 65
Figure 27. Block diagram of the measurement automation software (17) 66
Figure 28. PIM measurement results from a circuit combiner 79

1 INTRODUCTION

LM Ericsson has a long history in the field of telecommunications. LM Ericsson was started in 1876 in Stockholm, Sweden as a telegraph repair workshop by Lars Magnus Ericsson (13). Currently in 2014, LM Ericsson has over 110 000 employees internationally (9).

The networks section of LM Ericsson in Oulu was started in 2012. It is mainly concentrated on developing small-cell radio base station products. The small cells are part of the heterogeneous networks concept. Heterogeneous networks contain various cell sizes, ranging from large macro cells to very small cells. This helps to obtain a good throughput and user experience in heavily populated areas and indoors where dense macro network is impossible to build.

An efficient, high quality radio hardware is the backbone of a product utilizing radio frequencies (RF). The radio hardware consists of multiple components that must fit together to ensure effective transfer of data over the air. Also, several standards define how a product must perform, for example in terms of safety and electromagnetic compatibility (EMC). In addition, companies developing radio products often set their own internal performance requirements for their products.

While some data in RF hardware performance can be gained by simulations and component manufacturers test data, unexpected issues may occur with actual components. By carefully evaluating the components, both separately and in a line-up, these issues may be circumvented before the development has gone too far.

RF measurements done at a development phase differ from those done at a production phase. The measurements in development phase usually require more precision and accuracy, while the measurements at a production phase require fast results. Also, at a development phase measurement setups change often.

From earlier experience it was learned that doing complex measurements for a radio development manually took a great effort. Also, a simple human error during a measurement or calibration phase would lead to inaccurate results. Thus, it was found necessary to automate these measurements to as large degree as possible.

Five basic measurements are needed to evaluate the basic components of a radio transceiver. The main objective of this thesis was to automate these five measurements.

The measurement results obtained from an automated measurement must be as accurate as results obtained using a manual measurement. Also, the modularity of the automation software is a requirement and parts of software must be reusable. The results must also be in a format which is easy to process further. To automate these measurements, a study of the measurement and automation environment was required. This included the software used, interfaces and instrument control methods. This was the secondary objective.

This thesis also explains the basics of radio architectures and components as a background for the measurements. This is needed to ensure a high enough level of understanding of systems that are to be measured.

2 RF TRANSMITTER AND RECEIVER

Due to the diversity of components operating in radio frequencies, it was necessary to study the topic in detail in order to measure the components. An overview of general RF components and radio architectures is thus given in this thesis, in chapters 2 and 3.

RF transmitters and receivers are used, as the name implies, to transmit and receive electromagnetic waves at radio frequencies. A device which contains both a transmitter and a receiver for two-way communication is called a transceiver. There are multiple transceiver architectures.

The most commonly used radio architecture is a super-heterodyne transceiver, which utilizes an intermediate frequency (IF) as a step in both up- and down-conversion. A super-heterodyne transmitter first up-converts the transmitted baseband signal to an IF frequency and then to an RF frequency. At the receiver side, an input RF signal is first down-converted to an IF frequency, and then to the baseband. Multiple IF stages can be used if needed.

An IF frequency is often used in a transmitter and receiver because the components operating at higher frequencies are harder to manufacture and thus expensive compared to the ones operating at lower frequencies. The transmission of higher frequencies on printed circuit boards (PCBs) is also a difficulty, since PCB traces start to act as lossy matching components. In addition, filtering is easier at lower frequencies.

Another commonly used architecture is a direct-conversion radio transceiver architecture, also called a zero-IF transceiver. Direct-conversion converts RF frequencies directly to a baseband frequency, without the use of an IF frequency. The advantage of this is the simplicity of architecture, since fewer components are needed for the RF frontend. This leads to a lower power consumption. Also, filtering is simpler since instead of a band-pass channel filter a low-pass one can be used. The disadvantage of zero-IF architecture is performance, due to imperfections and nonlinearities in modulator components. These imperfec-

tions can be countered to some degree using software- and hardware-based corrections.

2.1 RF transmitter components

This example architecture is a direct conversion transmitter.

A typical RF transmitter used in telecommunications consists of a digital baseband which contains the modulator, digital-to-analog converter (DAC), local oscillator, mixer, variable gain amplifier (VGA) for setting the output power and power amplifier (PA). Also, in frequency domain duplexing systems, a duplex filter is used to isolate receiver (RX) and transmitter (TX) frequencies.

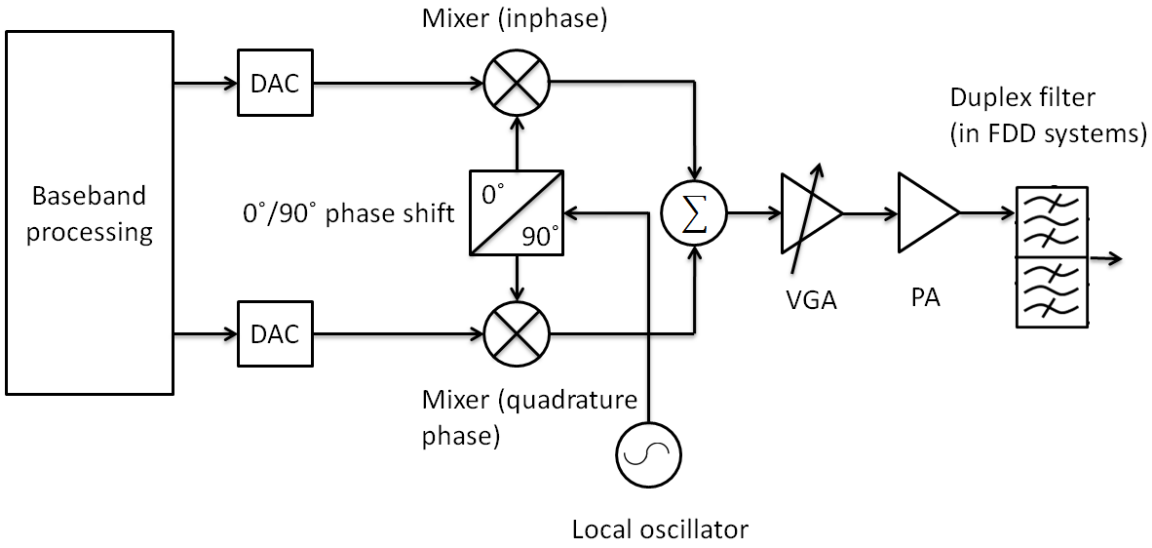

Figure 1. Block diagram of an example RF transmitter architecture (17)

2.1.1 Modulator

Most modern telecommunications devices utilize some form of quadrature amplitude modulation (QAM). In QAM, data is transmitted using the amplitude and phase properties of a signal. Modulation is usually done in a digital baseband, and data is processed into in-phase (I) and quadrature-phase (Q) branches.

Data bits vs. phase/amplitude in QAM can be represented using a constellation diagram:

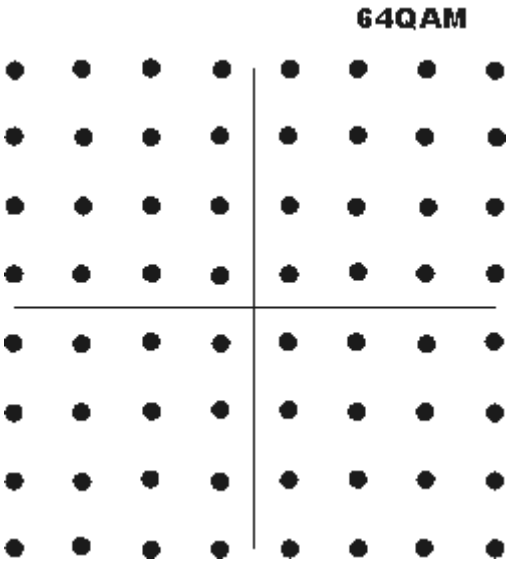

Figure 2. Example of a QAM constellation diagram (22)

In figure 2, each dot represents binary data. The length of the data in each constellation point is dependent on the order of QAM. A QAM signal can also be represented using complex numbers. In this case the in-phase (I) branch is represented as the real part and quadrature-phase (Q) branch as the imaginary part.

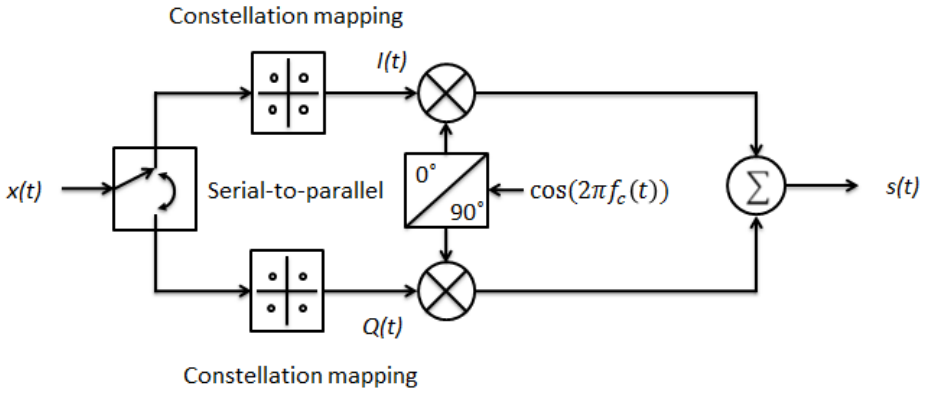

Figure 3. Block diagram of a QAM modulator (17)

In figure 3, a serial bit stream *x(t)* is converted to two parallel streams. These parallel streams are mapped into I- and Q-values depending on the constella-

tion used. A constellation mapper is basically an amplitude shift keying (ASK) modulator.

FORMULA 1. Output of a QAM modulator (34)

$$s(t) = Icos\big(2\pi f_c(t)\big) - Qsin(2\pi f_c(t))$$

Where

$s(t)$ = Time-variant output signal

I = In-phase signal amplitude

$f_c(t)$ = Time-variant carrier signal and

Q = Quadrature phase signal amplitude

Thus, due to the phase relations of sine and cosine, the two transmit branches are 90 degrees out of phase with one another.

In the example transmitter, both branches are converted into analog signals separately before summing them. This is called a complex-IF structure.

A local oscillator's signal is mixed directly to an in-phase transmit signal, and with 90 degrees phase shift to a quadrature phase transmit signal. After up-conversion, the two signals are summed. For modulator, the balance between I- and Q-branches is important. Since modulator components cannot be ideal, an imbalance between I- and Q-branches can have an effect on performance. To counter this imbalance, digital domain corrections can be made at constellation mapping or, for example, a DC offset may be added into the signal after digital-to-analog conversion.

2.1.2 Digital-to-analog converter

A digital-to-analog converter (DAC) converts a discrete-time digital domain value into a continuous analog amplitude. Once the transmitted data is mapped into QAM I- and Q, these two branches are converted into an analog signal

voltage. DAC has a certain resolution, in bits, defining its maximum input value and thus its dynamic range.

Also, output bandwidth of DAC is limited by its sample rate, as stated by Nyquist's theorem:

FORMULA 2.Nyquist's theorem (23)

$$f_s > 2f_i$$

Where

f_s = Sampling rate and

f_i = highest frequency component in information signal.

A converted analog signal can be either at an IF frequency, or a baseband frequency, depending on the used signal processing and the sample rate of the DAC. Because the DAC output is a stepped voltage, a reconstruction, or "smoothing" filter must be used in its output:

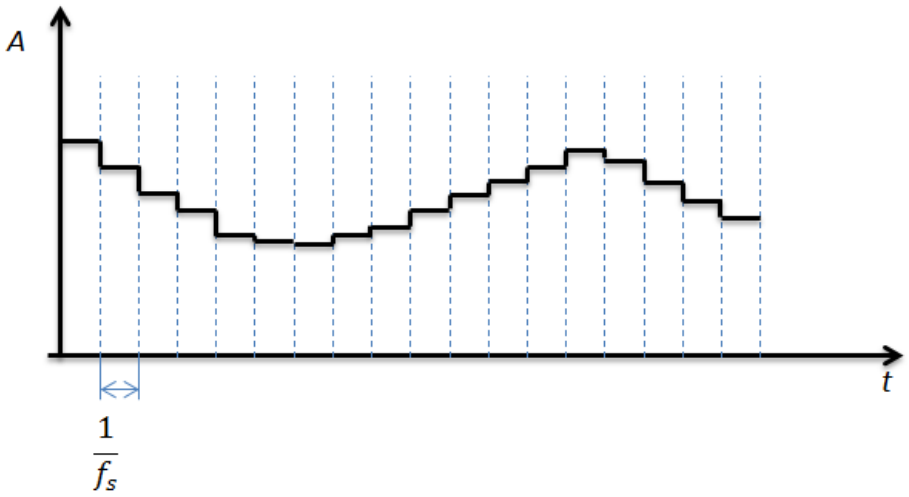

Figure 4. DAC output before a reconstruction filter (17)

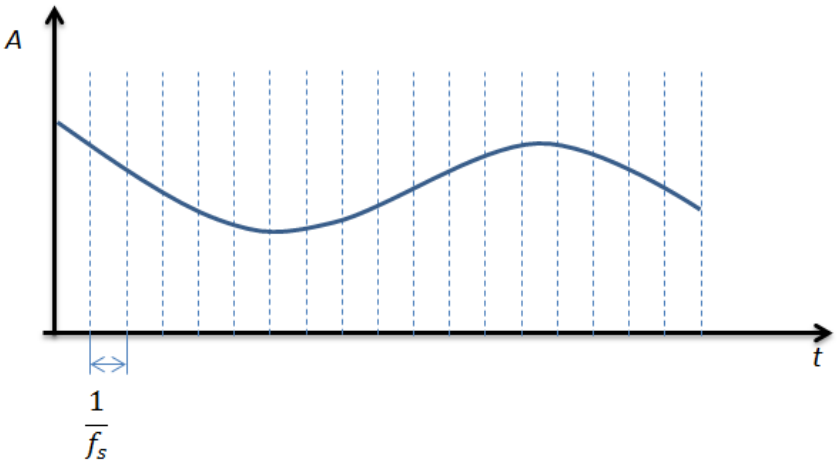

Figure 5. DAC output after a reconstruction filter (17)

In figures 4 and 5, the output of a DAC before and after the reconstruction filter is seen. The Y-axis contains the amplitude and the X-axis is time. The reconstruction filter is basically a simple low-pass filter, with a pass band edge frequency at the highest wanted frequency component at the DAC output.

2.1.3 Mixer

The mixer is used to up-convert the transmitted signal into the desired transmit frequency. The most basic mixer is a non-linear component, for example a diode. The mixer's output frequency is:

FORMULA 3.Output of a mixer (25)

$$f_{out} = |nf_1 \pm mf_2|$$

where

f_{out} = output signal,

f_1 , f_2 = two input signals

n, m = harmonic order from zero, which is the fundamental signal, to infinity

f_{out} = resulting output signal

An RF frequency synthesis (usually called a local oscillator in system level diagrams) is typically done using a phase locked loop (PLL), where an accurate reference oscillator is used to control a higher frequency voltage controlled oscillator (VCO). This VCO's output is fed back, its frequency is divided, and then it is compared to the reference oscillator. the phase difference of these signals is then used to control the VCO, to compensate for any phase shift. This also leads to a compensation of frequency drift, and thus the frequency and phase both stay "locked". The output frequency of PLL depends on the divider/dividers, and by changing them it can be varied.

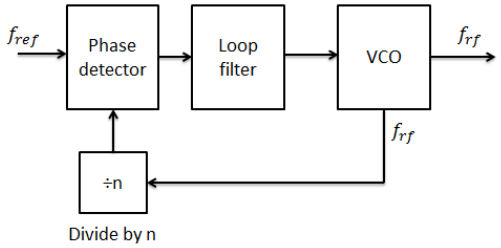

Figure 6. Simplified PLL architecture (17)

A transmit signal is then fed to amplification stages. There are multiple performance characteristics in both a modulator and mixer. Also, the local oscillator's performance is important, since it affects the performance of the whole system. Local oscillator's important performance characteristics include phase noise and frequency accuracy. In a mixer, the intermodulation characteristics, port isolation, noise factor and conversion loss/gain are often the most important performance parameters.

2.1.4 Variable gain amplifier and power amplifier

Since the transmitter's output power cannot be constant in most cases, it has to be controlled. A common way of controlling the output power is a separate variable gain amplifier. The gain of amplifier can be controlled by attenuating the input signal and by adjusting internal amplifier voltage levels, for example its biasing. The gain setting is usually controlled either by an external voltage setting or by a digital interface.

Important parameters of the VGA are its gain setting range and step size, bandwidth, linearity, efficiency and noise.

A power amplifier is the last amplifier stage in the transmitter. It is used to amplify the transmitted signal to the final transmit power. The most important performance parameters of a power amplifiers are linearity, power added efficiency (PAE) and noise. Also, harmonic distortions produced by the amplifier must be noted.

These parameters are explained more thoroughly in chapter 3.1.

2.1.5 Duplex filter

A duplex filter is used to isolate a transmission signal from a receiver input. It also has a function of attenuating unwanted spectral emissions and distortions generated by the device itself, and interference generated by other devices. As an example, the frequency response of Triquint 856931 duplex filter is seen in figures 7 and 8.

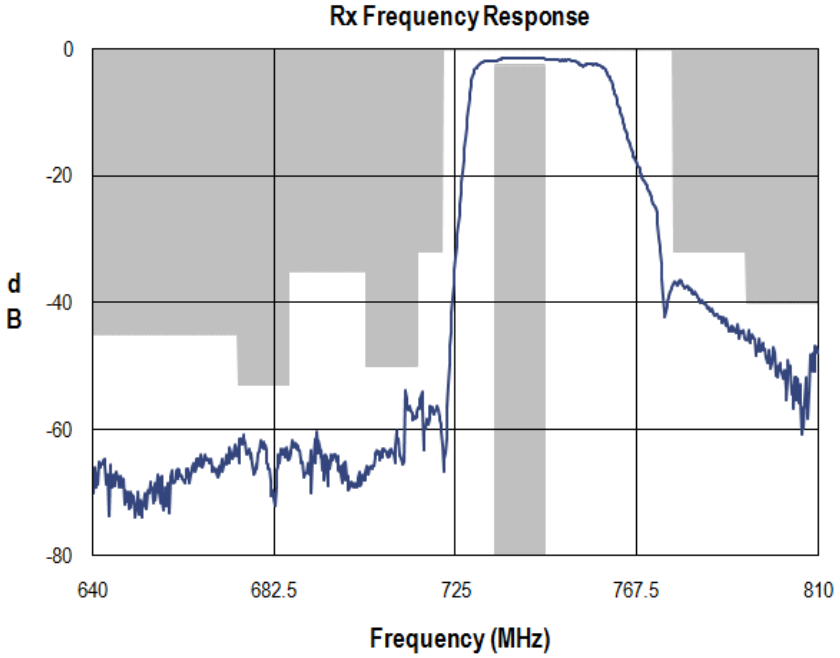

Figure 7. RX side frequency response of an example duplexer (32)

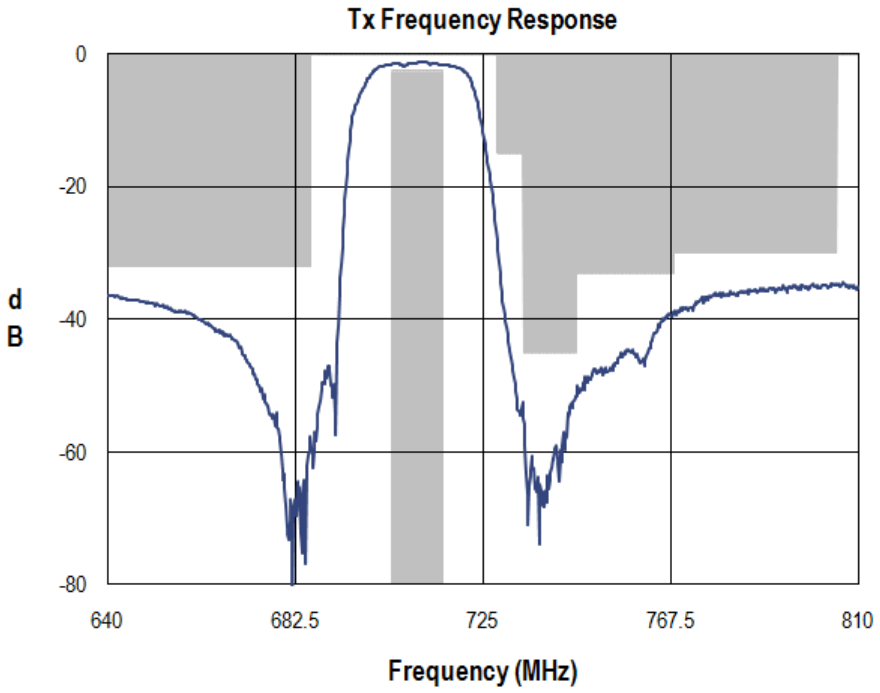

Figure 8. TX side frequency response of an example duplexer (32)

A typical duplex filter consists of two band-pass filters, with passbands at RX and TX frequencies. The important parameters of duplex filter's TX side include response in passband and stopband, matching, steepness and passive inter-modulation properties.

2.2 RF receiver components

This example receiver architecture is a direct-conversion receiver, with a separate quadrature demodulator.

A typical radio frequency receiver in telecommunications consists of a duplex filter in FDD systems, a low-noise amplifier (LNA), a mixer, a variable gain amplifier (VGA), an IF filter and an analog-to-digital converter (ADC).

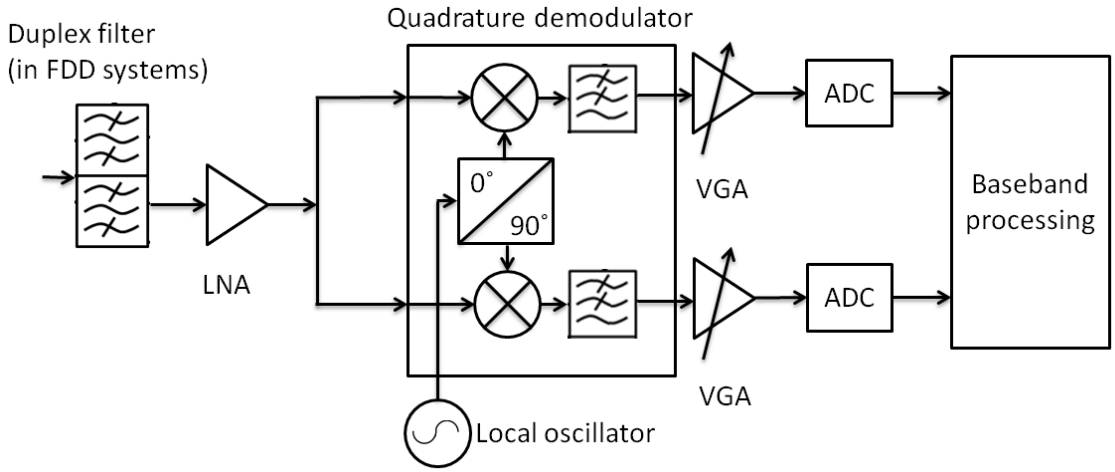

Figure 9. Block diagram of an example RF receiver architecture (17)

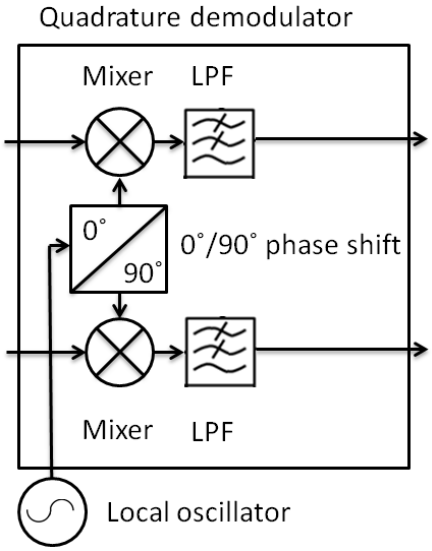

Figure 10. Block diagram of the quadrature demodulator used in the example receiver architecture (17)

2.2.1 Duplex filter

After a receiving antenna, signal is fed to a duplex filters receiver side. The isolation of transmitted signal from a received signal is an important factor of duplex filter's performance, since the power level of transmit signal is far greater than that of a received signal. Also, insertion loss of duplex filter is an important parameter, since the received signal is of low level. At receiver side of the duplexer, the power levels are far lower and passive intermodulation is usually not an issue.

2.2.2 LNA

A low noise amplifier is the first amplifier stage in a receiver. The first amplifier stage is the most dominant noise source, and thus its noise factor must be low. The amount of noise generated by a receiver immediately affects its sensitivity. Sensitivity and noise will be explained more thoroughly in chapter 3.3.

2.2.3 Quadrature demodulator

A signal demodulation can be done either fully in a digital domain, or partly in an analog domain. Demodulation is done by separating the I- and Q-branches of a received signal, making bit decisions based on amplitude values and multiplexing the results into a serial bit stream. The I- and Q-separation can be done either in an analog or a digital domain.

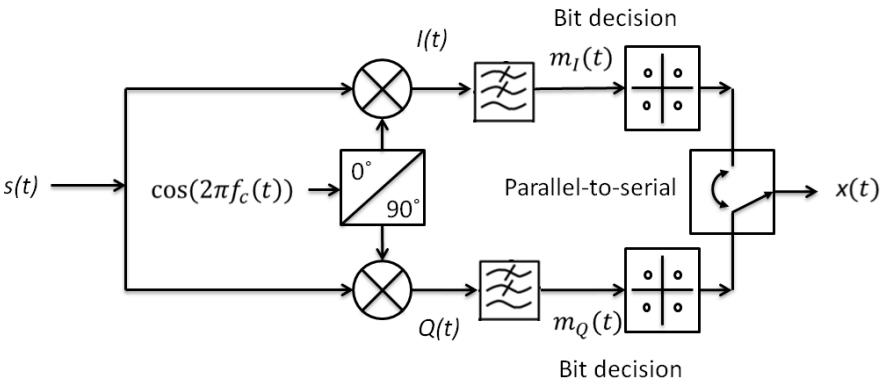

Figure 11. Block diagram of a QAM demodulator (17)

In figure 11, a generic architecture-level block diagram of QAM demodulator is seen. It consists of two multiplication (mixing) operations, phase shifter and two low-pass filters. After filtering, the amplitudes of I- and Q-branches are used to make the bit decisions. Basically, the decision is made using an ASK demodulator. Then, data is multiplexed into a serial format.

The mixing results of input signal $s(t)$ and the cosine signals $\cos(2\pi f_c(t))$ and its phase shifted variant $\cos(2\pi f_c(t) - 90°)$ can be seen in formulas 4 and 5:

FORMULA 4. QAM demodulator in-phase mixer output (20)

$I(t) = s(t)\cos(2\pi f_c(t))$ and

FORMULA 5. QAM demodulator quadrature-phase mixer output (20)

$Q(t) = s(t)\cos(2\pi f_c(t) - 90°)$
=

$Q(t) = s(t)\sin(2\pi f_c(t))$

where

$I(t)$ = time-variant in-phase branch of the input signal,

$Q(t)$ = time-variant quadrature phase branch of the input signal,

$s(t)$ = time variant input signal and

$f_c(t)$ = time-variant carrier frequency.

If the demodulator input signal $s(t)$ with message signals $m_I(t)$ and $m_Q(t)$ embedded, is defined to be:

FORMULA 6. Demodulator input signal with message signals

$s(t) = \ m_I(t)cos\big(2\pi f_c(t)\big) - m_Q(t)sin(2\pi f_c(t))$

where

$s(t)$ = time variant input signal,

$f_c(t)$ = time-variant carrier frequency,

$m_I(t)$ = time-variant in-phase message signal,

$m_Q(t)$ = time variant quadrature phase message signal,

the result of the multiplication becomes:

$$I(t) = \cos\left(2\pi f_c(t)\right) * \left(m_I(t)cos\left(2\pi f_c(t)\right) - m_Q(t)sin\left(2\pi f_c(t)\right)\right)$$

$$= \frac{1}{2}m_I(t) + \frac{1}{2}m_I(t)cos\left(4\pi f_c(t)\right) - \frac{1}{2}m_Q(t)sin\left(4\pi f_c(t)\right)$$

and

$$Q(t) = sin\left(2\pi f_c(t)\right) * \left(m_I(t)cos\left(2\pi f_c(t)\right) - m_Q(t)sin\left(2\pi f_c(t)\right)\right)$$

$$= -\frac{1}{2}m_Q(t) + \frac{1}{2}m_I(t)sin\left(4\pi f_c(t)\right) - \frac{1}{2}m_Q(t)cos\left(4\pi f_c(t)\right)$$

Then, the double frequency components $sin\left(4\pi f_c(t)\right)$ and $cos\left(4\pi f_c(t)\right)$ can be removed by low-pass filtering the signal and message signals $m_I(t)$ and $m_Q(t)$ are recovered. From these message signals the original data can then be recovered.

In this example, the branches are separated using a quadrature demodulator, which contains a mixer and low-pass filter. Then, these branches are converted to a digital domain using the ADC. Bit decision and parallel-to-serial conversion operations are done in the digital domain.

2.2.3.1 Mixer

A frequency down-conversion in a receiver mixer follows the same principles as in a transmitter mixer, explained in chapter 2.1.3. In the receiver used in this example, the mixer is integrated in the quadrature demodulator block and sum frequencies produced in mixing operation are filtered by the low-pass filter used. As with the LNA, the noise figure of mixer stage is very dominant in a total receiver noise figure.

2.2.3.2 Low-pass/IF filter

In this example the IF filtering is done using a simple low-pass filter (LPF) rather than a band-pass filter (BPF). This is due to the zero-IF architecture. Generally, an IF filter is used in the receiver to filter out frequency components that are outside the desired IF bandwidth. These include image frequency components produced in down-conversion. Also, an IF filter can be used for channel pre-selection to filter out adjacent channels which may induce blocking of wanted signal. This eases the need of additional digital filtering in a baseband processing.

2.2.4 VGA

A final amplifier stage, in this example receiver chain, is the variable gain amplifier. It is used to ensure that the analog-to-digital converter's input power level is within its dynamic range, preventing overflows. The received signals power must be measured to control the gain level.

2.2.5 Analog-to-digital converter

An analog-do-digital converter (ADC) converts a continuous-time analog amplitude into a discrete-time digital domain value.

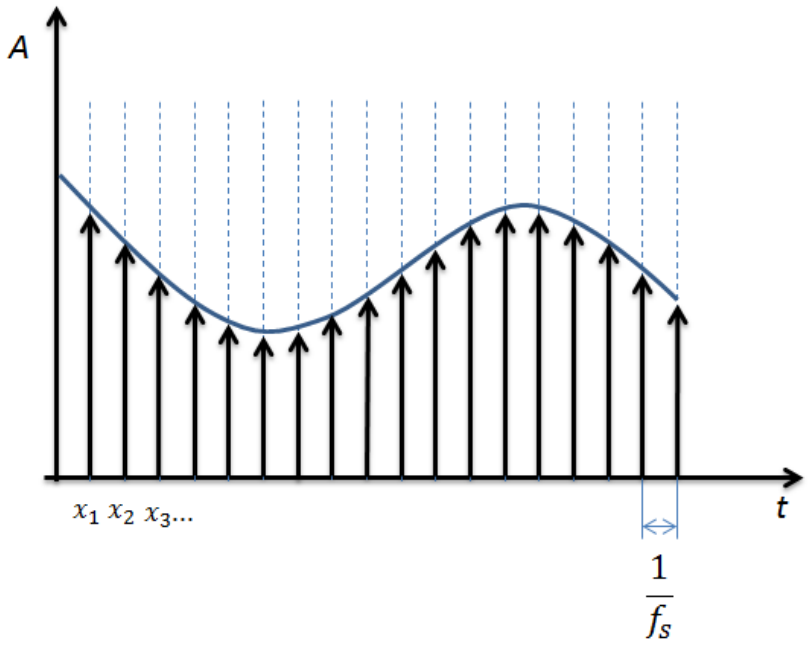

Figure 12. Illustration of ADC sampling of an analog signal (17)

In figure 12, an analog signal with time-variant amplitude A in blue trace is sampled at sample rate f_s. X-axis represents time. Samples $x_1, x_2, x_3 \dots x_n$ are digital amplitude values of the analog signal, with a time interval $\frac{1}{f_s}$ between samples.

As with DAC, the ADC has certain input level range and digital resolution in bits, which characterizes the largest amplitude value it can digitize. Also, a maximum sample rate of the ADC defines the maximum bandwidth of a converter, defined by Nyquist's theorem in equation 2.

3 RF TRANSCEIVER MEASUREMENTS

It was necessary to study the requirements, measurements and the background of them in order to develop automation. In this chapter, five important measurements defining the base performance of a radio device are explained. These five measurements are to be automated as the main objective of this thesis.

Devices operating in radio frequencies have multiple performance requirements and international regulations. These regulations include limitations to an output power and unwanted emissions.

The 3rd Generation Partnership Project (3GPP) has defined standards for telecommunications devices. The 3GPP consists of six different telecommunications standard development organizations (1). Thus, the standards defined by 3GPP are multinational, and most radio devices approved by these standards can be used all around the globe.

In addition to regulations, the components creating the baseline of the radio device must be compatible with each other. For example, choosing a nonlinear power amplifier generating wideband intermodulation distortion and a duplex filter with a low stop-band attenuation in 3GPP frequency band 2 (21) (RX at 1850 MHz – 1910 MHz, TX at 1930 MHz – 1990 MHz) can lead to a lower RX sensitivity. This is caused by the spectral regrowth generated in the nonlinear amplifier interfering with the receiver, due to the narrow 20 MHz spacing between RX and TX frequencies.

Also, power consumption has to be noted along with thermal characteristics. If the efficiency of transmitter is low and it requires special cooling to function, the development and implementation costs of the cooling are higher. In addition, the costs of running and maintaining the system are higher.

3.1 Linearity of the active transmitter components

The RF components used in telecommunications are non-ideal in nature. This means that the output of the system or component is not directly proportional to the input of the system or component. If a components output is directly proportional to its input, it is fully linear. As an example, the transfer function of a linear, ideal amplifier can be defined by formula 7:

FORMULA 7. Linear transfer function of an amplifier (15)

$$V_{out}(t) = GV_{in}(t)$$

Where

$V_{out}(t)$ = Time-variant output voltage of the amplifier,

G = Voltage gain of the amplifier and

$V_{in}(t)$ = Time-variant input voltage of the amplifier

To ease calculations, decibels (dB) are often used as units when characterizing amplifier gain levels and attenuations. Using decibels, the multiplication becomes summation. When characterizing power levels, a decibel relative to one milliwatt (dBm) is the most used unit. The power level in watts can be converted to dBm using the following formula:

FORMULA 8. Power in watts to a dBm conversion (26)

$$P[dBm] = 10\log_{10}(\frac{P[W]}{1\ mW})$$

where

$P[dBm]$ = Power in [dBm] and

$P[W]$ = power level in watts to convert into dBm.

Using decibels as the unit of power, the gain of an linear amplifier can be defined as:

FORMULA 9. Linear amplifier gain in decibels (10)

$$G = 10 \log_{10} \left(\frac{P_{out}}{P_{in}} \right) dB$$

Where

G = gain of the amplifier, in [dB]

P_{out} = output power of the amplifier, in [dBm] and

P_{in} = input power of the amplifier in [dBm].

Hence, a linear output power of an amplifier can be defined to be:

FORMULA 10. Linear output of an amplifier when decibels are used as units

$$P_{out} = P_{in} + G$$

where

P_{out} = output power of the amplifier in [dBm],

G = gain of the amplifier in [dB] and

P_{in} = input power of the amplifier in [dBm].

When a signal containing multiple frequency components is fed into a nonlinear system, the nonlinearity generates new spurious frequency content in addition to the input frequency content. These spurious frequency components are called the intermodulation (IM) distortions (IMD). The IM products are not to be confused with harmonics, which are integer multiples of an input signal.

Due to this the linearity is one of the most important factors when defining the performance of a transceiver, since the spurious content generated can cause interference issues in either the own radio system or the radio systems of others.

Nonlinearities are mostly caused by impurities, junctions of dissimilar substrates and resistive connections inside components. A nonlinear behavior can be modeled during a transceiver development and thus its effects on performance analyzed (*11*). For example, one way to model a nonlinear behavior of a component mathematically is to use a basic polynomial equation:

FORMULA 11. Polynomial equation (15)

$$V_{out}(t) = C_1 V_{in}(t) + C_2 V_{in}(t)^2 + C_3 V_{in}(t)^3 \ldots$$

where

$V_{in}(t)$ = Time-variant input voltage of the system

$V_{out}(t)$ = Time-variant output voltage of the system

C_1, C_2, C_3, C_4 = the polynomial coefficients of the nonlinear transfer function.

As an example of a nonlinear behavior, a generic MATLAB model was created for this thesis to simulate a spectral regrowth caused by intermodulation. The model is given a random complex input signal filtered with a channel filter (equivalent to real I/Q output signal of a QAM modulator) as a parameter, and it outputs the signal with nonlinear components added. The nonlinear model created can be expressed by the following odd-order polynomial equation:

FORMULA 12. Odd-order 7th degree polynomial equation

$$V_{out}(t) = C_1 V_{in}(t) + C_3 V_{in}(t)^3 + C_5 V_{in}(t)^5 + C_7 V_{in}(t)^7$$

where

$V_{in}(t)$ = Time-variant input voltage of the system

$V_{out}(t)$ = Time-variant output voltage of the system

C_1, C_3, C_5, C_7 = the polynomial coefficients of the nonlinear transfer function.

In the example equation, the modeled nonlinearities are odd-order. Even-order nonlinearities are often destructive in nature, and odd-order constructive. The MATLAB code for the nonlinear model is included in appendix 2.

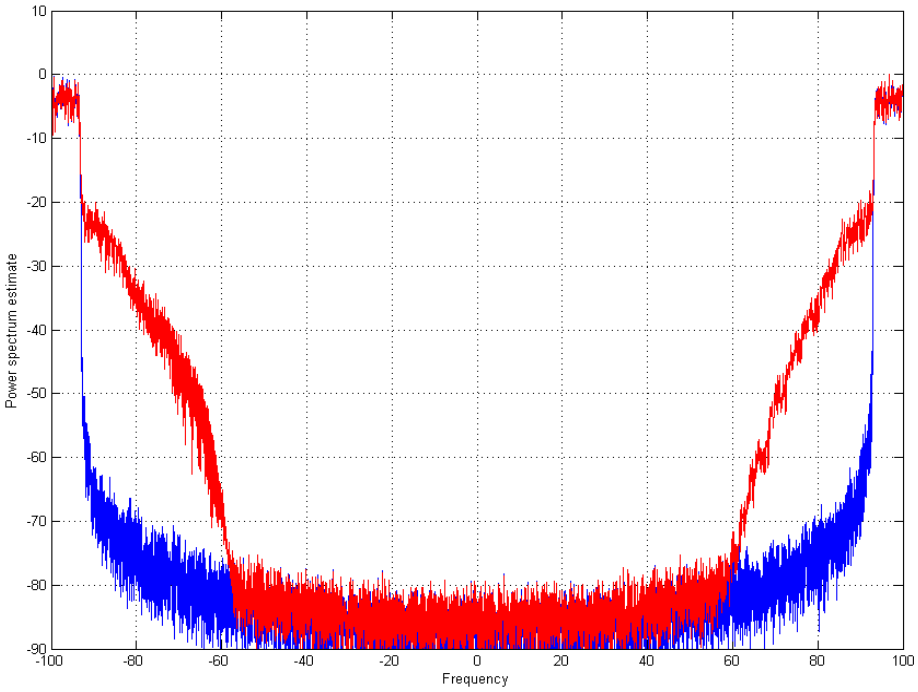

Figure 13. MATLAB power spectrum estimate of a wideband signal fed into generic nonlinear model (17)

In figure 13, the polynomial model in equation n. is used to characterize the effects of nonlinearity of a system. A blue trace represents the output power spectrum of a linear system and a red trace that of the nonlinear, modeled system. The spectral regrowth generated by the nonlinearity can clearly be seen in the red trace.

In addition to the high-order polynomial model, 3rd degree and 5th degree models were tested on a two tone input signal:

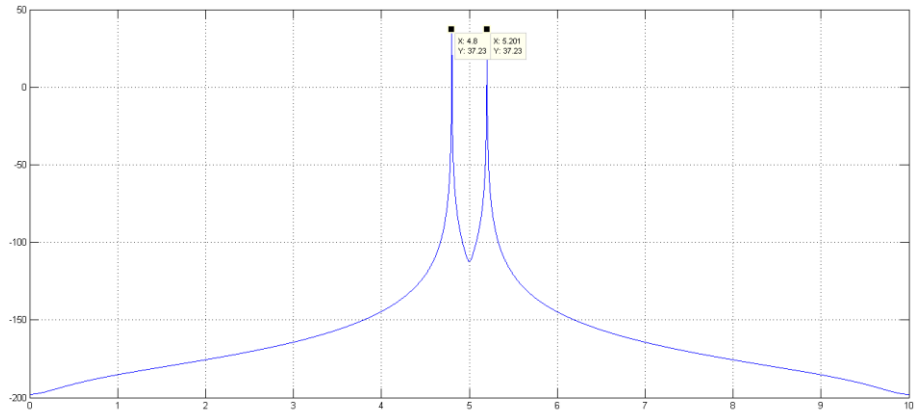

Figure 14. MATLAB plot of an original two-tone input signal (17)

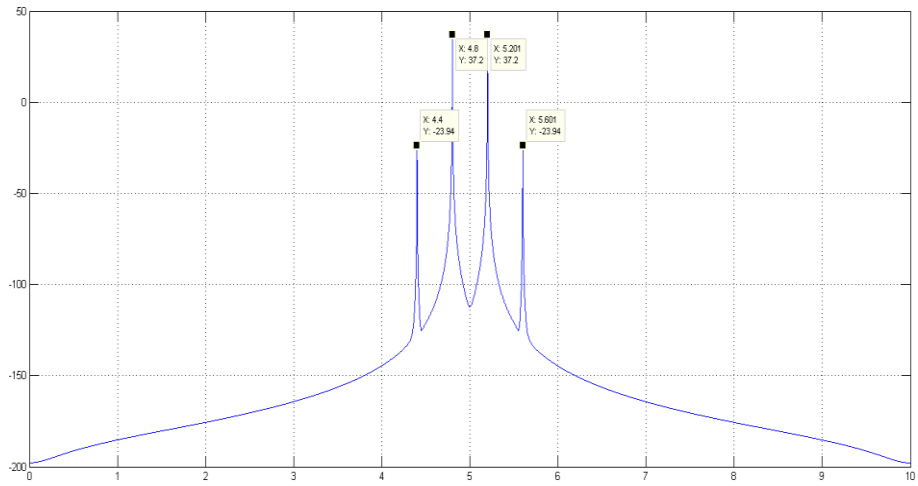

Figure 15. MATLAB plot of a 3rd degree model result (17)

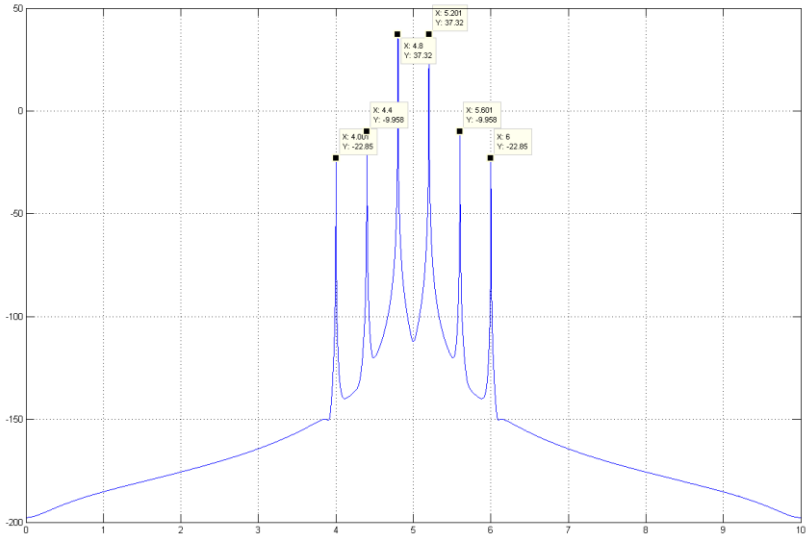

Figure 16. MATLAB plot of a 5th degree model result (17)

Thus, it can be seen that the degree of the polynomial has a direct effect on the nonlinearity content.

In general, most nonlinearities are caused by active components of the system. A passive intermodulation (PIM) also occurs due of same impurities and material junctions, but in a lesser extent. A passive intermodulation is explained more thoroughly in chapter 3.5.

In amplifiers, the gain is usually constant at small signal input power levels. When the input power is increased and the amplifier's output power level reaches a certain point, the gain starts to decrease. This is called a gain compression. In an ideal amplifier, gain compresses when an output signal's peak voltage reaches an amplifier's supply voltage. In real-life components, the gain compression is reached earlier due of threshold voltages and resistances inside components. After the gain has compressed by 1 dB, the operation of the amplifier has reached a point characterized as P1dB point. After this point, the gain typically begins to fall rapidly.

3rd order nonlinearities are often dominant in the system, thus they are used for a performance characterization. In general, a 1 dB rise in the input power raises

IM products of 3rd order by 3 dB. Using an amplifier's linear gain before P1dB, a theoretical point of interception between input/output and non-linear components can be calculated. This point is called an output 3rd order intercept point, OIP3. This intercept point is theoretical due to the gain compression.

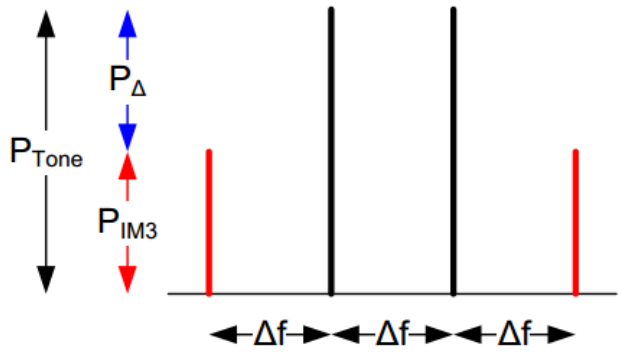

Figure 17. IMD3 frequencies (4).

The simplest way to measure a linearity of a component is to feed two CW tones, with separation Δf, into the device under test. Then, using a spectrum analyzer, generated IM products can be measured.

Usually, power levels of IM products ($P_{IMD}[dBm]$) are compared to the signal power ($P_{SIG}[dBm]$):

FORMULA 13. Calculating decibels relative to the carrier

$$P_{IM3}[dBc] = P_{SIG}[dBm] - P_{IM3}[dBm]$$

Where $P_{IM3}[dBc]$ is the IMD power, in decibels relative to the carrier,

$P_{IM3}[dBm]$ = IMD power in dBm and

$P_{SIG}[dBm]$ = wanted signal power in dBm.

As stated before, the nonlinearity of a component causes the output spectrum to expand into adjacent channels. This can lead to an interference in other services utilizing the radio spectrum. 3GPP has defined a limit for this adjacent

channel power, which is in case of LTE set to -45 dBc with all signal bandwidths (6).

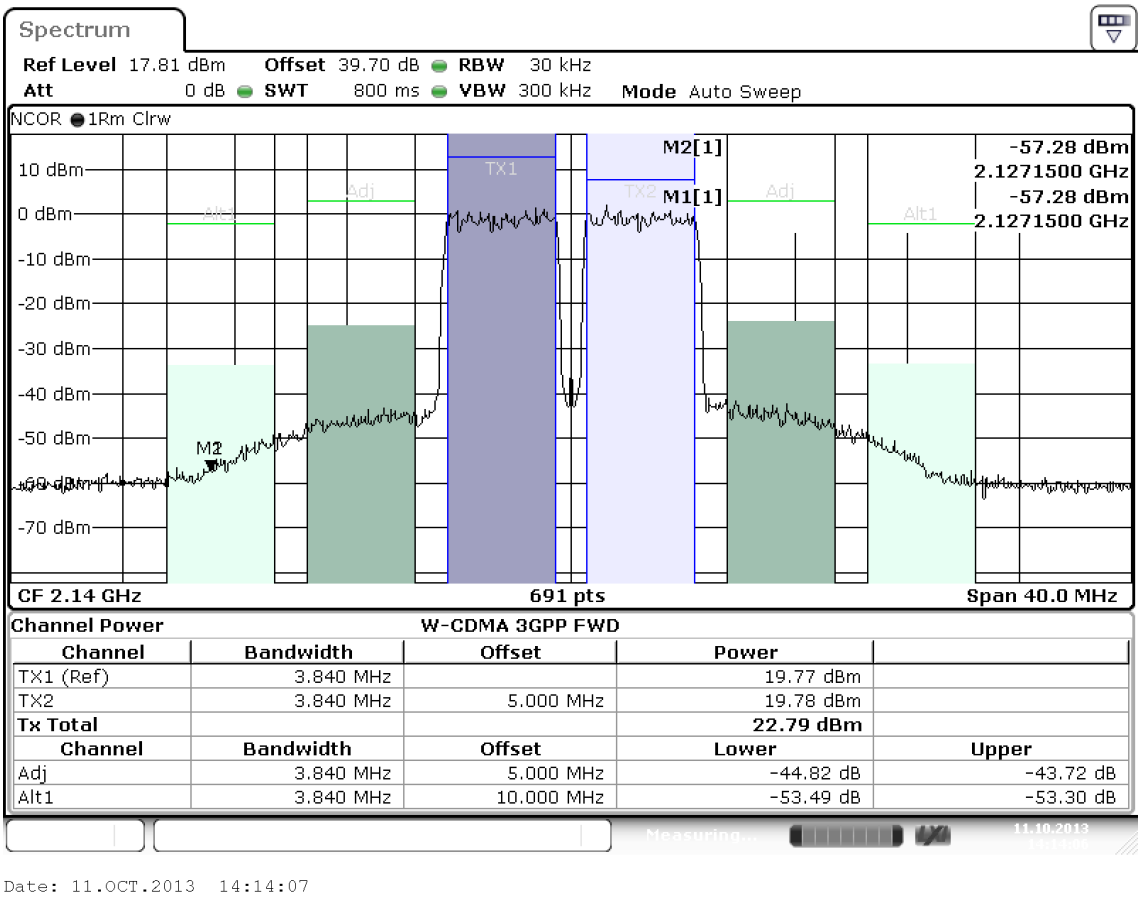

Picture 1. Screenshot of an adjacent channel power measurement (17)

In the screenshot seen in picture 1, a Rohde & Schwartz signal analyzer was used to measure the output power and adjacent channel power (ACP) of an instrumentation amplifier. The used test signal is a dual-carrier WCDMA signal. The instrument integrates signal powers over both carrier bandwidths which are 3,84 MHz, and displays the results in the channel power table below, in rows TX1 and TX2. The Tx Total row displays the power sum of both carriers. Two rows below contain the ACP results of an adjacent channel (Adj), which is at 5 MHz frequency offset from the nearest carrier and alternate channel (Alt1),which is at 10 MHz offset from the nearest carrier.

An adjacent channel power is integrated over the same 3,84 MHz bandwidth as the carriers. The ACP results are displayed in decibels relative to the carrier (dBc).

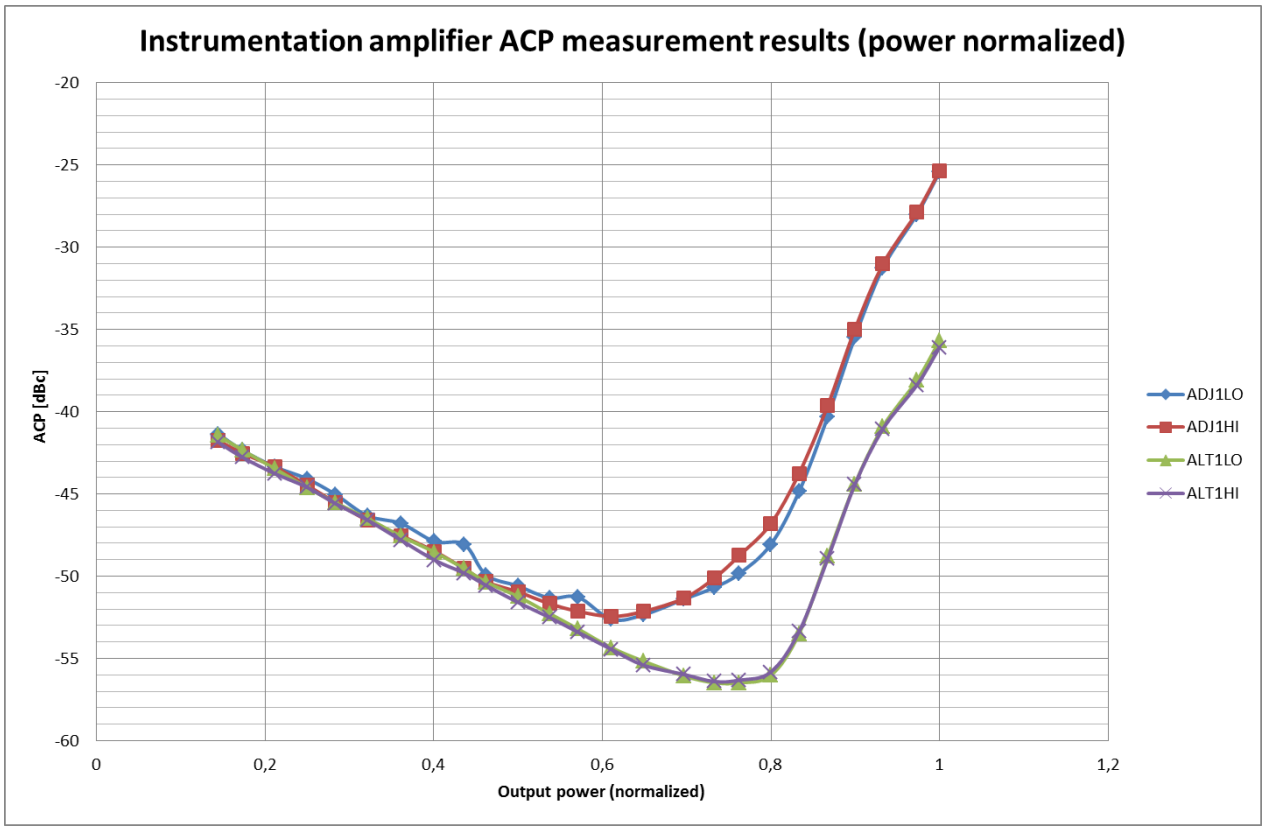

Figure 18. Example of amplifier measurement results, measured from a standard instrumentation amplifier (17)

If the test signal is of wide bandwidth, it may require special options in a spectrum analyzer instrument to integrate a power over signal and adjacent channel bandwidth separately. If such an option is not available, a carrier power and adjacent channel power can be calculated manually by measuring the power density (dBm/Hz) inside a desired signal bandwidth and integrating it over the whole measured signal bandwidth:

FORMULA 14.Calculating power over a certain bandwidth (18)

$$P_{wideband} = P_{density} + 10\log_{10}(BW)$$

Where

$P_{wideband}$ = Integrated power result over the desired bandwidth,

$P_{density}$ = power density and

BW = desired bandwidth.

If spectrum analyzers markers are used, the resulting power is usually integrated over the set resolution bandwidth (RBW). From this result, the wideband power can be calculated with:

FORMULA 15. Calculating bandwidth power when a certain resolution bandwidth is used in a measurement instrument (18)

$$P_{wideband} = P_{marker} + 10\log_{10}(\frac{BW}{RBW})$$

Where

$P_{wideband}$ = Integrated power result over the desired bandwidth,

P_{marker} = Marker power result

RBW = set resolution bandwidth of the spectrum analyzer

BW = desired bandwidth.

3.2 Power added efficiency

Another important parameter in any active component, for example an amplifier, is its efficiency. In short, efficiency describes how large a portion of input energy is transferred to the actual output signal, and how large portion is dissipated as heat. In an RF amplifier's case, efficiency is usually expressed with a power added efficiency (PAE):

FORMULA 16. Power added efficiency formula (3)

$$PAE\ [\%] = \frac{P_{out_{rf}} \text{-} P_{in_{rf}}}{P_{dc}} \cdot 100\%$$

Where

$PAE\ [\%]$ = power added efficiency,

P_{out_rf} = total RF output power of the amplifier in watts,

P_{in_rf} = total RF input power of the amplifier in watts,

P_{dc} = DC power fed into the amplifier, in watts.

The typical PAE values of amplifiers differ, due to different biasing and technologies. Also, components in the amplifiers matching and biasing circuit have an effect on PAE. When characterizing the efficiency of a single, discrete field effect transistor (FET), a drain efficiency is often used:

FORMULA 17. Drain efficiency of a transistor (6)

$$\eta_d[\%] = \frac{P_{out_{rf}}}{P_{dc}} \cdot 100\%$$

where

$\eta_d[\%]$ = drain efficiency percentage

P_{out_rf} = total RF output power of the amplifier in watts and

P_{dc} = DC power fed into the amplifier in watts.

A collector efficiency of a bipolar transistor is calculated using the same equation. For example, a class-B biased amplifier can theoretically have the maximum drain efficiency of 78,5 % (5). Since the drain efficiency equation does not take the input power into account, using the PAE calculation to determine the efficiency of RF amplifier is more accurate. However, it should be noted that as the gain of the amplifier increases, the effect of the input power to the efficiency decreases. At a certain point, the effect becomes minimal.

For example, in an amplifier that has the gain of 33 dB, the input power of 0 dBm, the output power of 33 dBm and DC power consumption of 8 W, the difference between a calculated drain efficiency and PAE is:

$$\eta_d[\%] = \frac{\frac{10^{\left(\frac{33}{10}\right)}}{1000}}{8} \cdot 100\% \approx 24{,}94\%$$

and

$$PAE\ [\%] = \frac{\frac{10^{\left(\frac{33}{10}\right)}}{1000} - \frac{10^{\left(\frac{0}{10}\right)}}{1000}}{P_{dc}} \cdot 100\% \approx 24{,}92\%$$

Thus, the difference is $0{,}02\%$ between the drain efficiency and power added efficiency**.**

A heat generation is always a problem in electronics, since too high temperature levels will cause the components to age faster, thus leading to shorter lifespans and lower reliability. Also, designing and implementing efficient cooling systems is expensive. Low PAE also leads to a higher DC power consumption, and the power supply for the amplifier must be designed accordingly.

PAE is an important factor in designing of all radio devices, from small battery powered devices to high power transmitters. In a battery powered device, a good PAE value leads to a longer operation time with battery power. In a high power transmitter, power consumption and cooling requirements can vary greatly even with a small change of PAE.

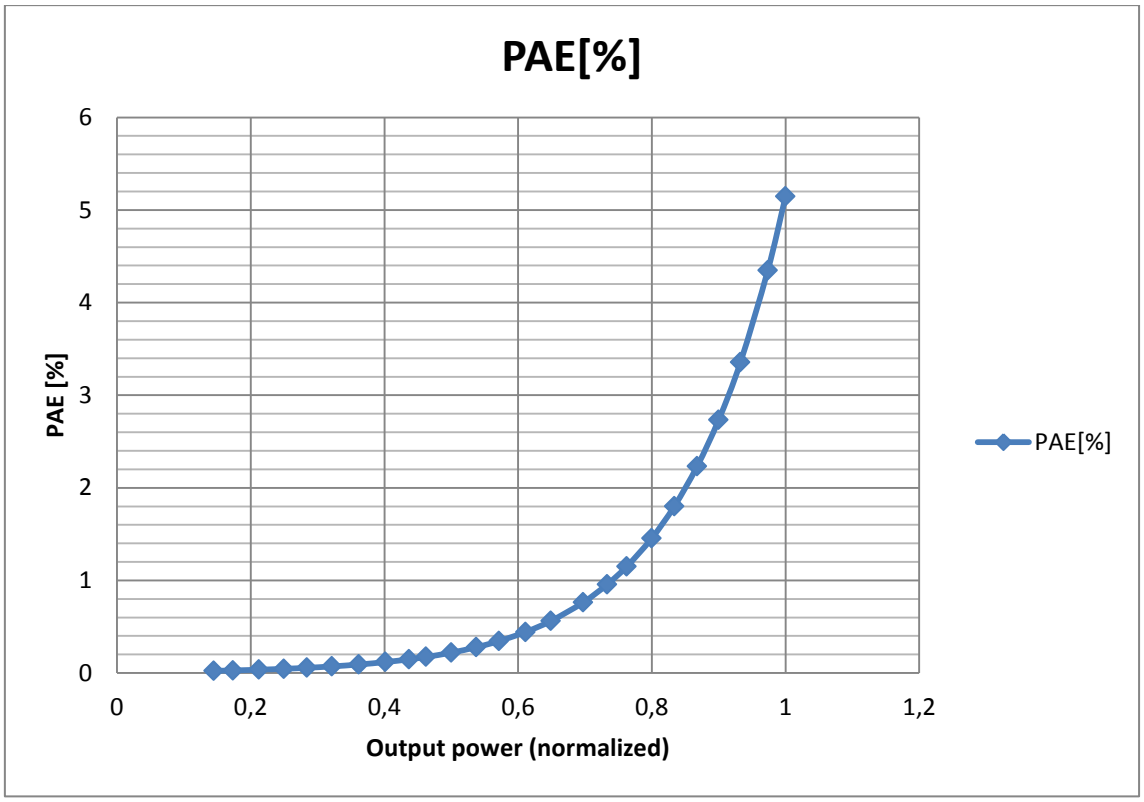

Figure 19. Example of a power added efficiency measurement result, measured from a standard instrumentation amplifier (17)

The power added efficiency can be measured using multiple techniques. One requirement in measurements is a signal source. A test signal is fed into the amplifier and the input power is measured by power meter or spectrum analyzer. In amplifier's DC input, both DC current and voltage are measured. At amplifier's output, power can be measured using a power meter or a spectrum analyzer. In general, PAE varies over the input power if the amplifiers biasing voltage levels remain constant.

Since even small errors in the measurement can affect the result, great care must be taken when calibrating the losses of the measurement circuitry.

3.3 Receiver sensitivity

The sensitivity of a receiver characterizes its ability to receive low-level signals and separate them from noise. The receiver sensitivity is limited by the thermal noise floor and a total noise figure of the receiver chain. The total noise figure (NF) is the sum of noise power produced by all components and elements in the

receiver chain. All active radio components used in electronics generate radio frequency noise by several mechanisms. For the receiver to detect a digitally modulated signal correctly, a certain signal-to-noise ratio is required at a de-modulator input. Thus, the sensitivity of a receiver can be defined by formula 18:

FORMULA 18. Calculation of the sensitivity of a receiver (18)

$$P_{sens} = P_{noise} + SNR_{min} + NF$$

Where

P_{sens} = receiver sensitivity limit,

P_{noise} = noise power level,

SNR_{min} = minimum signal-to-noise ratio for reception and

NF = total noise figure of the receiver.

If a spread spectrum system, for example a wideband code domain multiple access (WCDMA) is used, a signal can be received even if its power level is lower than the noise floor of the receiver. This is due to the process gain from the spectral spreading/de-spreading operation. The sensitivity limit of a receiver utilizing spread spectrum can thus be defined by the following formula:

FORMULA 19. Calculation of the sensitivity of a receiver when a spread spectrum is used (18)

$$P_{sens} = P_{noise} + SNR_{min} - PG + NF$$

Where

P_{sens} = receiver sensitivity limit,

P_{noise} = noise power level,

SNR_{min} = minimum signal-to-noise ratio for reception,

PG = process gain from de-spreading and

NF = total noise figure of the receiver.

3.4 Receiver adjacent channel selectivity

An adjacent channel selectivity of a receiver characterizes its ability to separate a low level wanted signal in presence of a higher level unwanted signal, which can also be called a blocker signal.

A real life blocking situation can happen for example when two mobile phones are close to a base transceiver station 1, henceforth called BTS1, and user equipment 1, henceforth called UE1 is connected to it. UE2 is connected to the BTS2, which is farther away.

These use cases happen more often in modern cellular networks utilizing overlay networks containing a multitude of different cell sizes, ranging from large macro cells to very small cells. These different base stations and cells are further defined by 3GPP standards (14).

Both mobile phones use WCDMA in a same frequency band 1, where a maximum output power is defined to be +24 dBm, and a minimum power -50 dBm (9). The transmit frequency of the UE is between 1920 MHz – 1980 MHz.

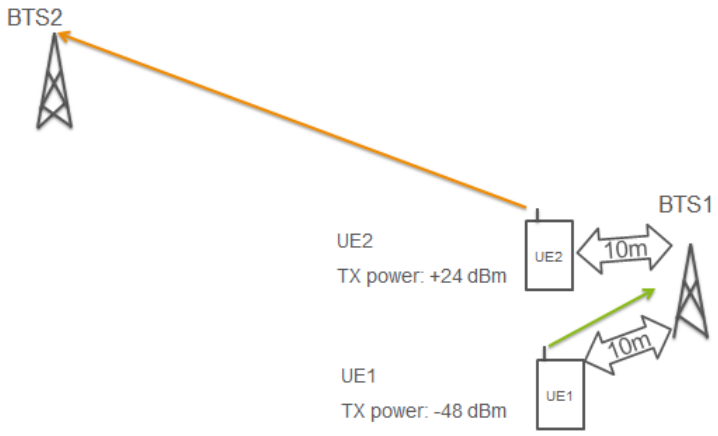

Picture 2. Example case (17)

A radio wave loses power when propagating in free space. This path loss is defined as:

FORMULA 20. Path loss in free space (24)

$$L = 20\,log_{10}\left(\frac{\lambda}{4\pi d}\right)$$

where

L = path loss (dB)

λ = wavelength (m)

d = distance between transmitter and receiver (m)

Due to the need to compensate for this path loss, the transmission power of UE2 is set to maximum (+24 dBm). UE1 is closer to BTS it is connected, thus its output power is set, for example, to -48 dBm.

Assuming that both mobile phones are located 10m from BTS1, and both the mobiles and BTSs have a zero antenna gain, an approximate path loss at ~2 GHz can be calculated by:

$$L = 20\,log_{10}\left(\frac{\lambda}{4\pi d}\right)$$

where

$$\lambda = \frac{C}{f} = \frac{300000\ km/s}{2\ GHz} = 0{,}15m$$

and

$$d = 10\ m$$

hence:

$$L = 20\,log_{10}\left(\frac{0{,}15\ m}{4\pi * 10\ m}\right) = -58{,}4623 \ldots dB$$

An approximate path loss attenuation is:

$L \approx -58\ dB$

Hence, received power in the BTS1 receiver is:

$P_{UE1} + L = -48\ dBm - 58\ dB = -106\ \mathrm{dBm}$

and

$P_{UE2} + L = 24\ dBm - 58\ dB = -34\ \mathrm{dBm}$

A required minimum dynamic range is:

$-106\ \mathrm{dBm} - (-34\ \mathrm{dBm}) = 72\mathrm{dB}$

Thus, the BTS1 receiver needs to have a dynamic range of over 72 dB. Also, the SNR requirement of a wanted signal must be met, extending the dynamic range requirement by the SNR. Since the ADC has a certain input resolution, a VGA is used to control the input power level to prevent overflow situations, as in the example in chapter 2.2. If the VGA is adjusted to lower its gain due to a blocking signal, a low level wanted signal may become indistinguishable from the noise.

In the absence of internal measurement software in a receiver, there must be a way to capture the ADC data of a receiver in order to measure the selectivity. From this ADC data, a power spectrum estimate can be calculated by the Fourier transform.

From the calculated power spectrum, a wanted signal power level can be compared to noise floor in order to determine if the wanted signal can be distinguished. Thus, the sensitivity of a receiver is measured in presence of a blocking signal. This measurement is then repeated using multiple blocker levels to define a total receiver dynamic range in different situations.

3.5 Linearity of passive components

Although most of the intermodulation distortions produced in an RF system originate from its active elements, also its passive components, transmission lines

and connections produce them. This passive intermodulation (PIM) has to be noted in a transceiver design, since its effects cannot be countered using the same methods as in its counterpart produced by active systems. This is due to the number of mechanisms producing the distortion, which makes modeling harder.

PIM is produced by metal-to-metal connections, impurities, contaminants and ferromagnetic materials. Additionally, electro-thermal conductivity effects have been identified as a major cause of PIM (35).

To measure a passive intermodulation, two CW signals are amplified to the needed power level, combined and fed to the passive component under measurement.

The power levels of passive intermodulation distortions are very low; hence a very high dynamic range in the measurement circuit is needed. This dynamic range requirement can exceed 100 dB, depending on the PIM production of the component measured. Usually normal RF measurement instruments, such as spectrum analyzers, cannot meet this requirement. An external circuitry can be used to extend the dynamic range, for example a signal feed-forwarding or filtering can be used to attenuate the used CW signals before the analyzer instrument.

As an example, four resonator filters with a tunable stopband are used in a circuit to improve the measurement circuit's dynamic range. First, two filters are used to attenuate the non-linear components produced by the circuit. They are connected to the circuit before a measured component, and tuned to frequencies obtained from formulas 21 and 22:

FORMULA 21. IMD frequency 1 calculation

$$f_{imd31} = |2f_{cw1} - f_{cw2}|$$

and

FORMULA 22. IMD frequency 2 calculation

$$f_{imd32} = |2f_{cw2} - f_{cw1}|$$

where

f_{imd31}, f_{imd32} are the IMD3 frequencies and

f_{cw1}, f_{cw2} are the CW frequencies.

At the measured components output, another two filters are connected to attenuate CW signals before the spectrum analyzer. This improves the dynamic range of the analyzer instrument, and low level intermodulation products can be measured. A spectrum analyzer should be set to a narrow frequency span and the resolution bandwidth adjusted to as narrow as possible for accurate results. In addition, a calibration of circuitry must be done with care.

4 OVERVIEW OF A MEASUREMENT AND AUTOMATION ENVIRONMENT

As stated in chapter 1, manually measuring components and complex systems were evaluated slow and inefficient. Also, a human error presented an uncertainty to the results. Thus, it was decided to automate these measurements. This is the main objective of this thesis. It is necessary to study and understand the software development environment chosen, the interfaces needed and the measurement instruments that were to be controlled by automation. Additionally, the calibration requirements of measurement circuits had to be taken into account.

National Instruments LabVIEW was used in a student project in Ericsson Oulu during spring 2013 to automate several RF measurements, and the feedback gained from these results was the main reason for choosing LabVIEW as a development environment. Also, many instrument manufacturers provide free-of-charge drivers for use with LabVIEW. These drivers, along with their documentation, make automation software development easier and faster. An easy generation of graphical user interfaces (GUI) was also noted as an advantage.

4.1 About LabVIEW

Control software which is developed with LabVIEW is called a virtual instrument (VI). A VI consists of two parts, the front panel which is the GUI visible to the user and the block diagram which contains the software functionalities:

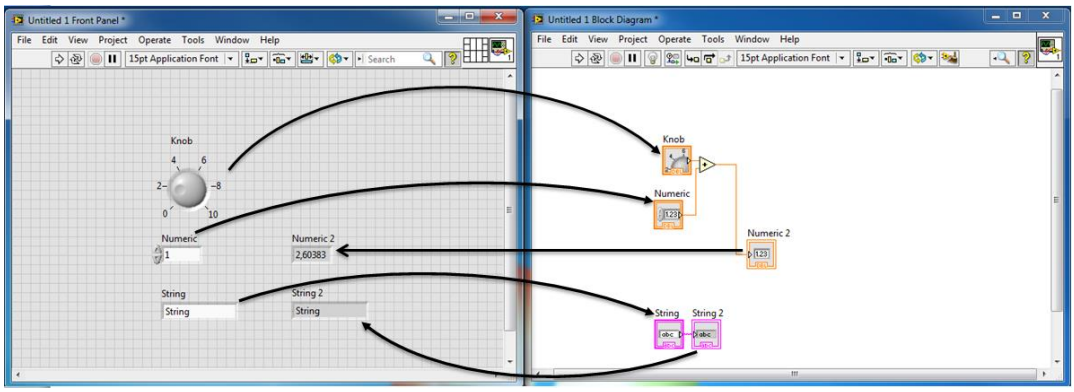

Picture 3. Example of relations between a front panel and a block diagram (17)

The front panel of a VI consists of controls and indicators. Controls are used to input variables to the software. Indicators are used to read and show output variables. There are also special controls and indicators. These include for example the resource names for connected instruments and LabVIEW error handling.

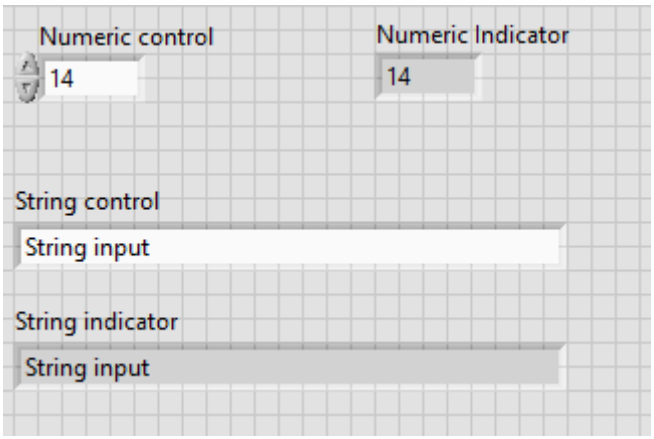

Picture 4. LabVIEW front panel example with controls and indicators (17)

In a block diagram, the items added into the front panel can be seen and connected to different operations by wiring. Also, the data types of items can be seen in icons. As a general development rule the program's execution should flow from left to right.

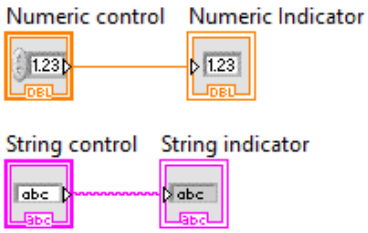

Picture 5. Block diagram linked to a front panel example in picture 5 (17)

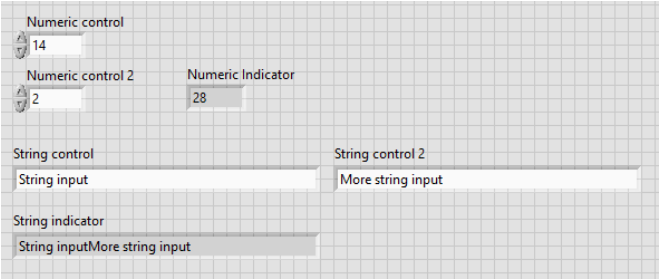

Picture 6. Example front panel with multiplication and ASCII string concatenation operations done in a block diagram (17)

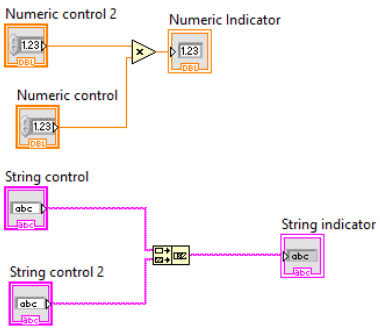

Picture 7. Block diagram with multiplication and string concatenation operations, linked to the front panel example in picture 6 (17)

All VIs developed can be used as subroutines which are called sub-VIs in LabVIEW. If a parameter or parameters need to be passed in or out of this sub-VI, it is possible to connect controls and indicators into the I/O terminals seen in the front panel. These I/O terminals can be seen at the upper right corner of the front panel development window, next to the icon of the VI. The VI icon can also be modified. As a general rule during development of software with LabVIEW, input terminals should be located on the left side of the icon, and the output terminals on the right side. These Sub-VIs can then be added to a block diagram of another VI. This enables a creation of higher level software executing and controlling multiple lower level sub-VIs. This is illustrated in pictures 8 and 10 below.

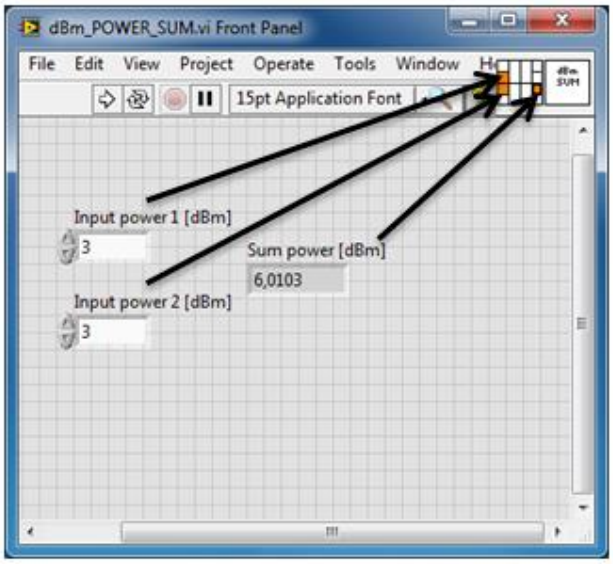

Picture 8. Example of linking controls and indicators into the VI I/O terminals (17)

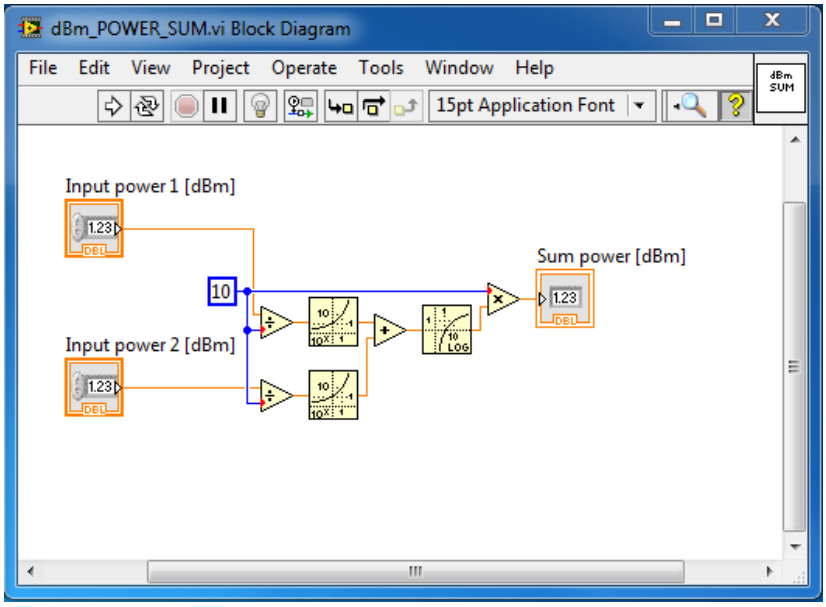

Picture 9. Block diagram of the sub-VI example in picture 8 (17)

This example VI seen in pictures 8 and 9 calculates the sum of two power levels given in dBm. When used as a sub-VI, these power levels are given as input and the sum is output from the VI:

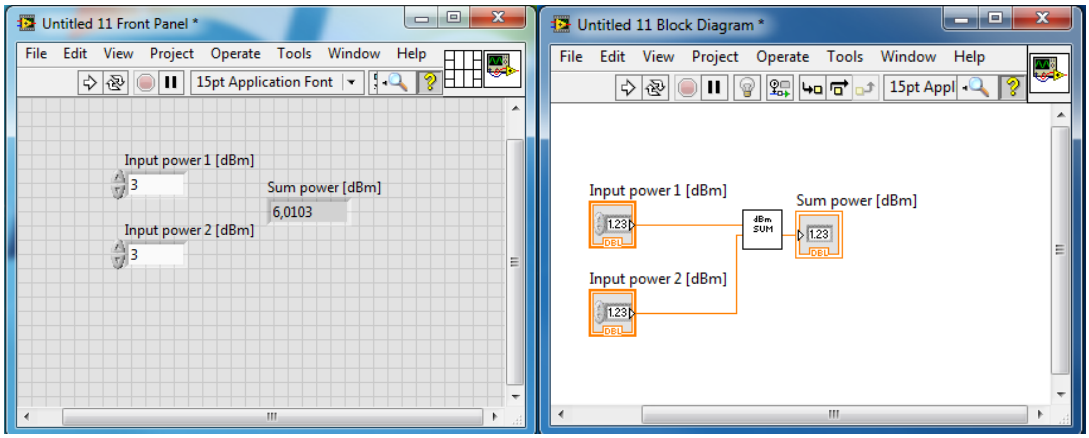

Picture 10. Example of a sub-VI usage. (17)

The use of sub-VIs keeps a complex software readable and more modular. Additionally, modifications done in sub-VIs are updated into the higher level VIs utilizing them.

The execution order of a VI or VIs is defined by a LabVIEW error line. LabVIEW also supports threading and parallel execution of operations, but these functionalities were not needed in the development of the thesis software.

Typically, in the development of LabVIEW VIs, the execution flows from left to right. Also, VI inputs are located on the left side, and outputs on the right side.

4.2 Overview of an example measurement system

In addition to normal RF measurement instruments, the device under test (DUT) needed to be controlled. An overview of one of the developed systems is seen below in figure 20.

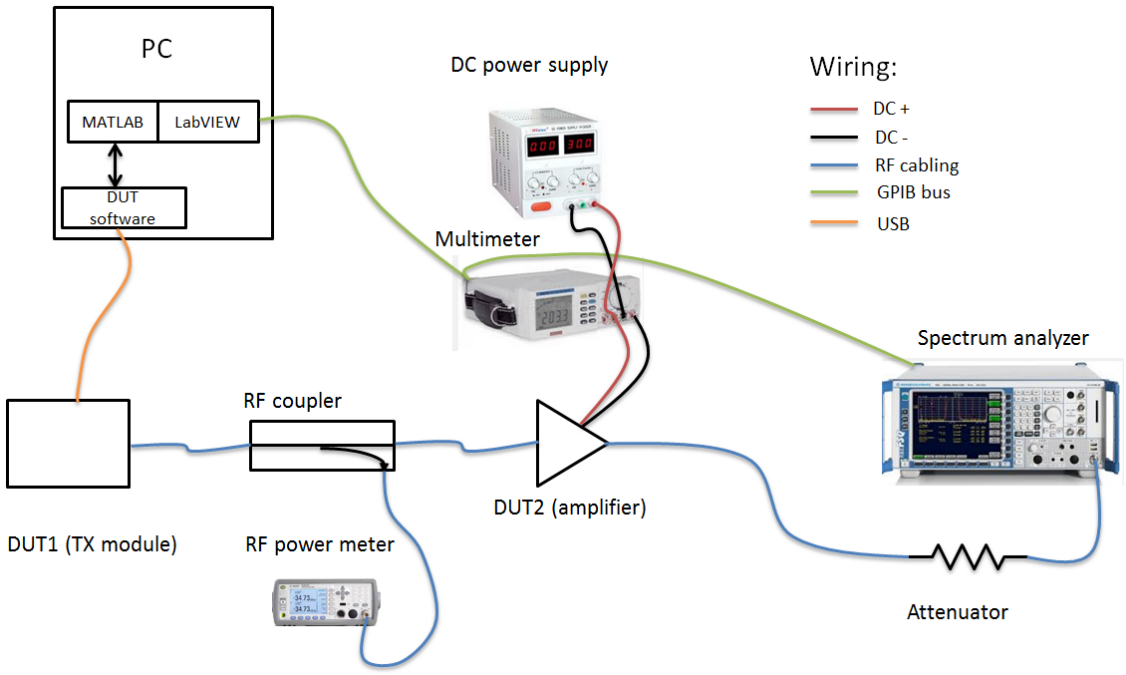

Figure 20. Example measurement system (17)

The measurement system in figure 20 contains two devices under test. A first device (DUT1) is a transmitter (TX) module and a second device (DUT2) is an amplifier. A controlling PC has a LabVIEW-based automation software controlling the system as whole, while MATLAB controls the TX module through a manufacturer-specific software interface. LabVIEW controls the instruments directly by methods further explained in chapter 4.3. MATLAB processing and control is integrated to a LabVIEW automation software, by interfaces explained in chapter 4.4.

The developed measurement system is used for a PAE measurement defined in chapter 3.2, by using a power meter, multimeter and spectrum analyzer. Additionally, the linearity of components in the system is measured with this setup using the spectrum analyzer as defined in chapter 3.1. The measurement results are gathered into a controlling PC for further processing and analysis.

Manual measurements after assembling the circuitry include only the calibration of attenuation losses from DUT2 input to the power meter input, which can be defined as:

FORMULA 23. Power meter offset calculation

$$L_{in} = L_{cr} - L_{il} - L_{cable}$$

where

L_{in} = total loss in dB,

L_{cr} = loss from coupler input to coupled port, coupling ratio in dB

L_{il} = insertion loss from coupler input to coupler output,

L_{cable} = attenuation of the cable from coupler to DUT2 input.

By setting the total loss L as offset into a power meter, the correct DUT2 input power can be measured. Offset can also be added afterwards into the results obtained from power meter.

Also, the losses from DUT2 output to a spectrum analyzer input must be calibrated. This loss is defined as:

FORMULA 24. Spectrum analyzer offset calculation

$$L_{out} = L_{cable1} + L_{att} + L_{cable2}$$

where

L_{out}= total loss in dB,

L_{att} = attenuation of the attenuator between DUT2 and spectrum analyzer in the setup

L_{cable1} and L_{cable2} = losses from cabling; from DUT2 to attenuator and from attenuator to spectrum analyzer.

The first instrument to control with automation developed was a network analyzer, used to measure different RF filters. Automation was used to measure

and store multiple different parameters in different environments. In total, the controlled instruments included the following:

- Network analyzer
- Signal generator
- Signal analyzer
- Power meter
- Multimeter
- DC power supply
- Programmable attenuator

4.3 Instrument control methods

All used instruments were controlled via a general purpose interface bus (GPIB), with the exception of a programmable attenuator which only had an RS232 and local area network (LAN) connectivity. In future, it is possible to upgrade the measurement system to utilize a LAN-based LXI system, with few instrument upgrades. This may become relevant in the future, since the GPIB bus has a limitation of total 15 connected devices at one time.

4.3.1 GPIB interface

The control of instruments connected by GPIB is done using the standard commands for programmable instruments (SCPI), through a virtual instrument software architecture (VISA) interface. GPIB is specified in the standard IEEE-488. GPIB devices can be connected to one of two topologies in terms of cabling: star or linear (31). These topologies are shown in figures 21 and 22.

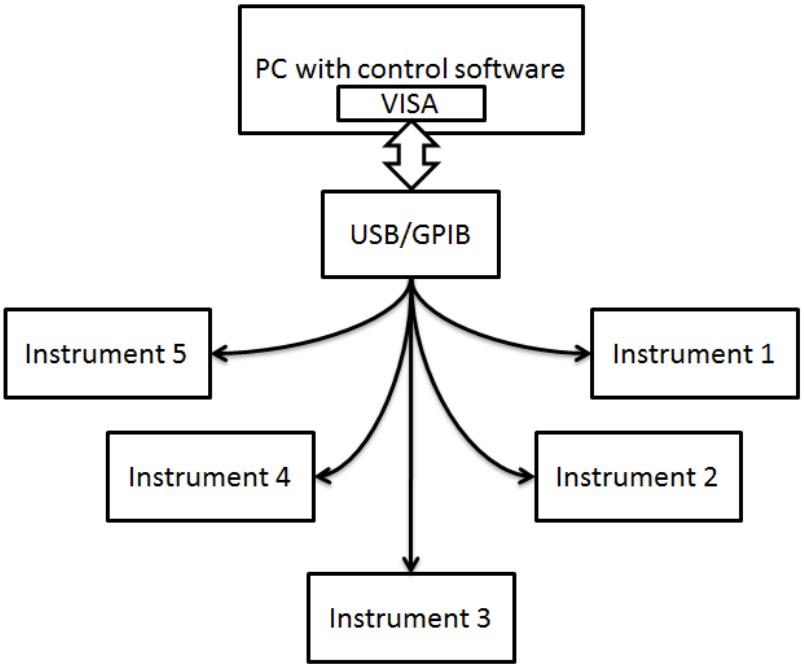

Figure 21. Star cabling topology defined in standard (17)

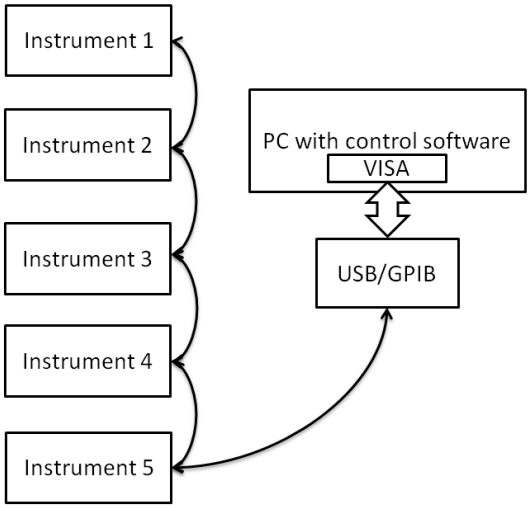

Figure 22. Linear, "daisy chain" GPIB topology used in a developed measurement automation (17)

There are 24 pins in the standard connector used for GPIB – eight for data I/O, five for bus management, three for handshaking and eight ground lines. A GPIB protocol supports three types of devices: controllers, talkers and listeners (12).

The controller monitors the communication in the network, and handles connections between talkers and listeners. The controller is usually the computer controlling the system.

A talker is a device which sends data to the network, while a listener is a device which receives data. Typically connected instruments are capable of both talking and listening functions. For example, when the controller is querying an instrument for data, the instrument is first a listener and when sending the result for query, it becomes a talker.

The commands to instruments are also standardized to some point. Standard Commands for Programmable Instruments (SCPI) define syntaxes of instrument control commands. These commands are ASCII-strings sent through the GPIB bus.

4.3.2 VISA software control interface

VISA is a high level I/O language calling lower level driver routines (16). An advantage of this is the use of same operations to communicate with instruments and control them regardless of the interface. This enables the use of same software whether the instrument is connected through for example USB, LXI or GPIB. Also, software using VISA function calls is easily portable between platforms. For example, a program written in C language using VISA can be ported to any other platform supporting C language.

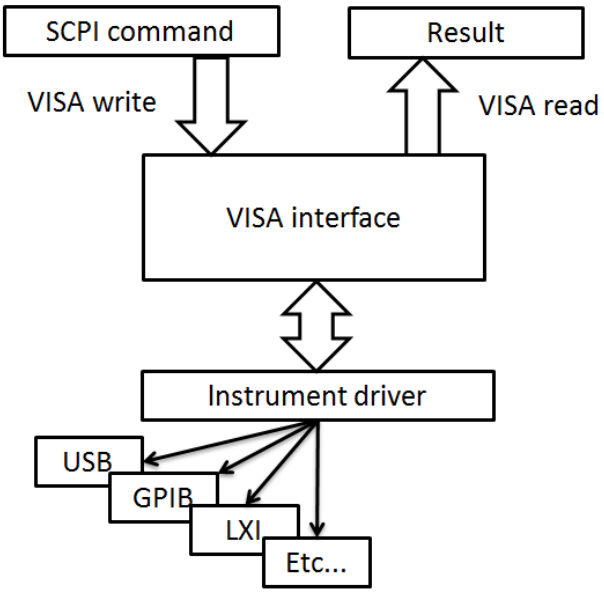

Figure 23. Illustration of a VISA interface data flow (17)

LabVIEW has several VISA operations in Instrument I/O-palette. The most important operations are VISA Write and VISA Read. VISA Write is used to send SCPI commands, and VISA Read is used to read query results. All VISA operations require the VISA resource name of a device controlled to be defined. LabVIEW scans for connected and installed devices automatically when a Refresh-button in a VISA resource name-control is clicked.

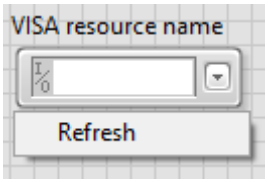

Picture 11. VISA resource name control in LabVIEW with a drop-down menu opened (17)

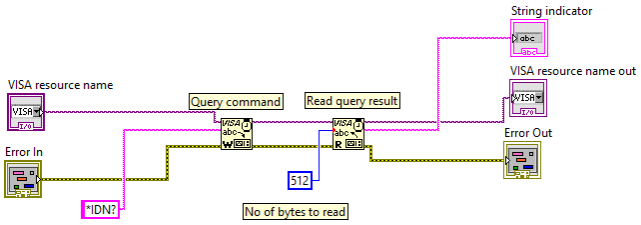

Picture 12. Example of a simple VISA query (17)

In picture 12, an SCPI query command “*IDN?” is written to a VISA resource name specified. VISA read then reads the query result, to a maximum of 512 bytes in size. If the size of the result is larger than 512 bytes, the part exceeding the read size defined is not read, usually generating an error message. All VISA reads return ASCII strings as a result, thus the format must be manually converted if needed. Since an error line defines the execution order, the query command is always executed before the read in this example.

While some control functionalities could be found in the instruments manufacturer’s LabVIEW drivers, some features needed to be added using the manufacturer’s specified SCPI control commands. Usually, the syntax for these commands could be found in the user manual of the instrument. These added commands were made into sub-VIs for an easy future use.

In the developed software, multiple feedback loops were required. This means that the settings of device under test (DUT) were changed according to its output:

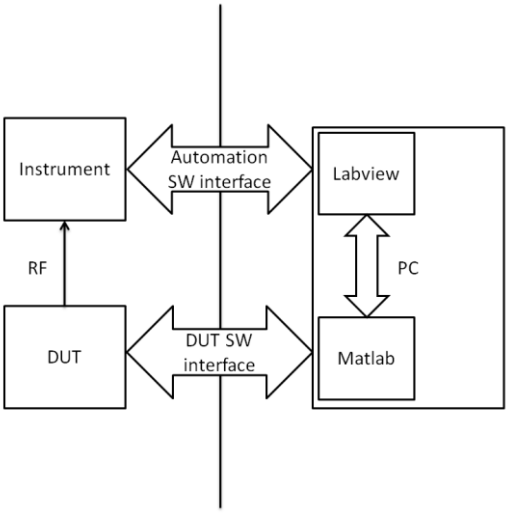

Figure 24. *Example of a feedback loop used in a measurement automation (17)*

The software integrations are explained in chapter 4.4.

4.3.3 Instrument control problems during development

During the first phases of development and testing, most of the problems were related to the timing of SCPI commands and VISA I/O operations. The timing and synchronization problems were overcome by using the operation complete (*OPC?) query. The OPC query reads the bit 0 of IEEE 488.2 defined status byte register in the instrument (33). This bit 0 is set high when all operations are completed.

Also, it was noted that regional settings of a controller PC were important. When generating SCPI commands to instruments that contain floating point numerical data, an incorrect decimal separator will lead to wrong actions in an instrument. Most controlled instruments read an integer part of floating point data correctly and a fractional part was not recognized if the decimal separator was wrong. When reading data from an instrument, it was also important to convert floating point numbers to a controller's regional format. If the read data was not con-

verted correctly, LabVIEW lost the fractional part. This led to incomplete results and, if the data was used to do controlling operations, possible crashes of software.

4.4 Software integrations and interfaces

In addition to LabVIEW, other software was needed in order to get the necessary results, and process them. The first versions of automation generated files that were used in other software, for example MATLAB. This slowed down the processing of results.

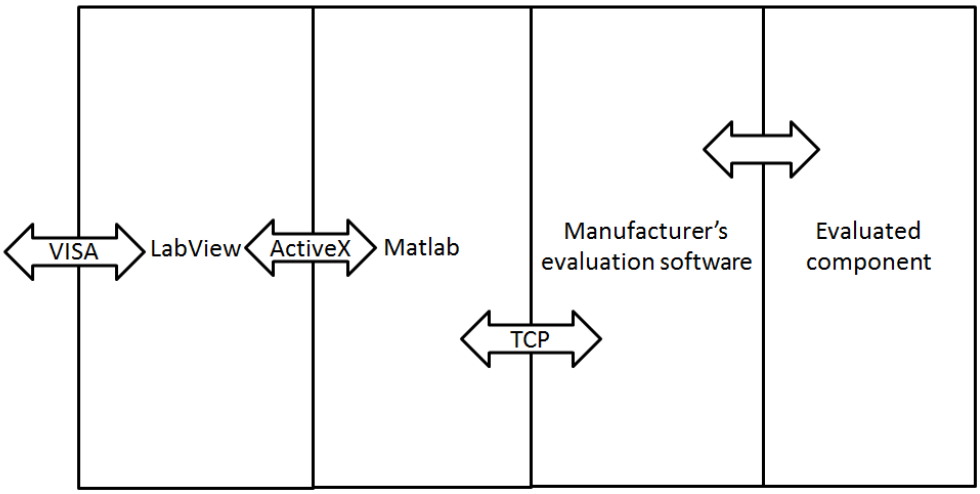

Figure 25. Example of software integration interfaces (17)

Also, some pre-existing signal processing functions were written in a MATLAB code, and importing them to LabVIEW was not feasible. A solution for this was found in LabVIEW documentation (19). A special MATLAB Script Node was used to pass data between LabVIEW and MATLAB through an ActiveX interface. Using this, LabVIEW could pass commands and data to a MATLAB workspace, and read variables from a MATLAB workspace. The use of a MATLAB Script Node required MATLAB to be installed and an active MATLAB license. The script node started a separate instance of MATLAB, executed the code specified and terminated the instance. Thus, workspace paths were needed to be defined in the node.

Some evaluated components were connected to the controlling PC by a USB interface, and they were controlled by using software provided by the component manufacturer. In some cases, the control of these components was automated. While the component manufacturers provided application programming interfaces (APIs) to automatize some features, not all functionalities were covered by existing APIs. The needed functionalities were added either by scripting or by MATLAB functions.

Usually the component manufacturers provided software to manually control the evaluated component. For automation, the APIs provided usually controlled the software used for manual control. This was accomplished by running, for example, a transmission control protocol (TCP) server in the controlling application and using the APIs to send commands to this server. The controlling software then translated these commands to the component in control.

4.4.1 Software integration example

Software integration was successfully used in both RX and TX measurement VIs. LabVIEW was used to control the instruments used in both measurements, and MATLAB was used to control the device under test.

In automated RX measurements, MATLAB was used to calculate measurement results from ADC data and to pass these results to LabVIEW. LabVIEW was then used to write these results to Excel sheets in a hard disk. This was done to avoid using very large arrays in both LabVIEW and MATLAB during the measurement, which lasted for several hours. In case of a software crash, these arrays of data could have been lost.

After the completion of the measurement MATLAB was first used to import these Excel files into arrays. Then, a noise correction is calculated and data was plotted to define a receiver performance in measurement situations.

4.4.2 Problems related in software integration

When controlling MATLAB using LabVIEW, multiple problems were encountered.

A malfunctioning ActiveX link was the most severe of them. This did not produce error message in LabVIEW unless data was passed between them and VI executed correctly without running any MATLAB scripts. This led to an incomplete measurement on multiple occasions. An ActiveX link between MATLAB and LabVIEW was also not initialized if LabVIEW was already running when an ActiveX server was started in MATLAB. The solution for this was to start ActiveX server before starting LabVIEW. If the link severed during measurement for some reason, both programs had to be restarted.

Also, a software bug related to DDE was found in MATLAB running on 64-bit Windows 7. If the DDE channel was initialized exactly 64 times during the script execution, the initialization failed. This produced an error message in MATLAB, but the error was not passed on to LabVIEW. The only found solution for the bug was to restart MATLAB; clearing the MATLAB workspace did not remove the problem.

5 AUTOMATION SOFTWARE FOR PASSIVE INTERMODULATION MEASUREMENTS

A passive intermodulation measurement case was chosen as the first example to illustrate how the automation software works. The second example is a power amplifier measurement automation, described in chapter 6. Three other automation software routines were developed for this thesis, but they are not explained in detail. This example VI contains similar features as other developed VIs, excluding a MATLAB integration, which is explained in chapter 4.4.

5.1 Measurement system

The measurement system for a passive intermodulation measurement consists of a signal source, two amplifies, RF combiner, two tunable resonator filters and a spectrum analyzer.

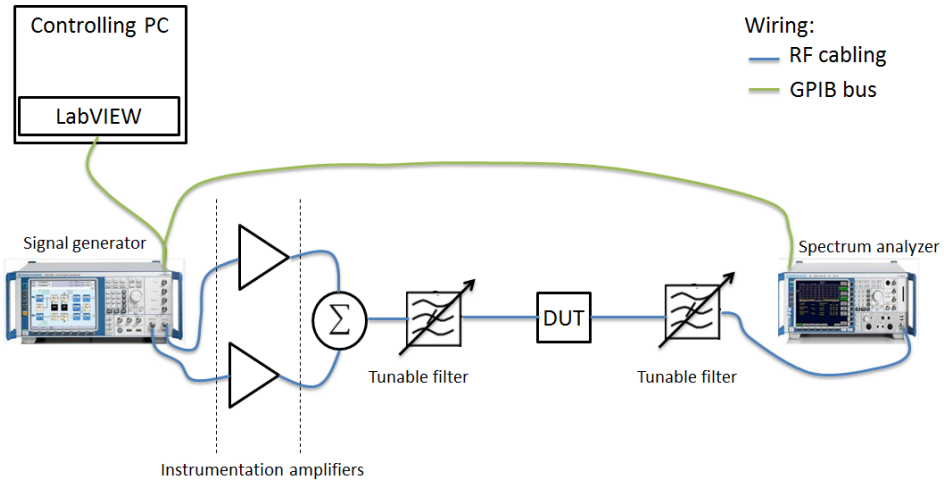

Figure 26. Illustration of the measurement system used for a passive intermodulation measurement (17)

In the measurement system illustrated in figure 27, a two-output signal generator is used as a signal source. The output signals are then amplified and combined. Then, a tunable resonator filter is used to remove the intermodulation distortion components produced by this circuit. In an ideal case, only two CW signals from a signal generator are input to the DUT. In reality, the circuit produces low but noticeable IM distortions, which must be removed. Depending on

the phase of these IM distortions, they can either add or decrease the measured IMD of the DUT. After the DUT, a second tunable resonator filter is used to attenuate the CW signals. This ensures that the spectrum analyzers mixer level is low enough to get the necessary dynamic range. Rohde & Schwartz FSV13 spectrum analyzer has a dynamic range of 73 dB in WCDMA ACLR measurements according to the product brochure (29). In case of CW signals, the dynamic range was not disclosed in the manual or datasheet.

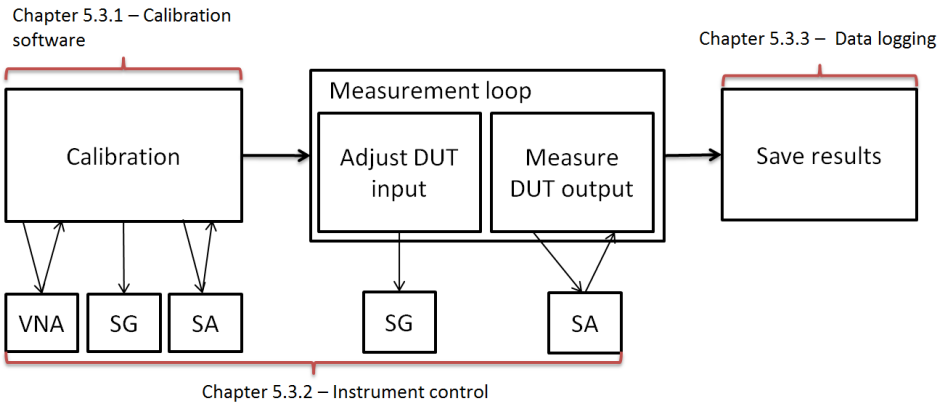

Figure 27. Block diagram of the measurement automation software (17)

The measurement system is controlled using a PC and LabVIEW-based software developed. First, a calibration offset is calculated for the spectrum analyzer using the vector network analyzer. Then, a constant power signal at low level is output from the signal generator. Using this constant power signal and the calibrated offset, the gain of amplifiers used in system and losses in circuits can be calculated.

When the calibration of a path signal generator-DUT is finished, a starting power level can be set in a signal generator. The software executes a downwards power sweep in 1 dB steps. The starting power level is the maximum input power of the DUT, which is user-definable. The number of steps is also user-definable.

5.2 User interface of passive intermodulation measurement software

To ease the use of measurement automation, all control of the software was bundled under a single user interface. The user interface contains multiple controls and indicators:

- Measurement parameters
- Result destination
- Measurement status
- I/O settings
- Results of the current iteration
- Calibration data and execution
- LabVIEW error clusters

This UI can be seen in picture 13 below.

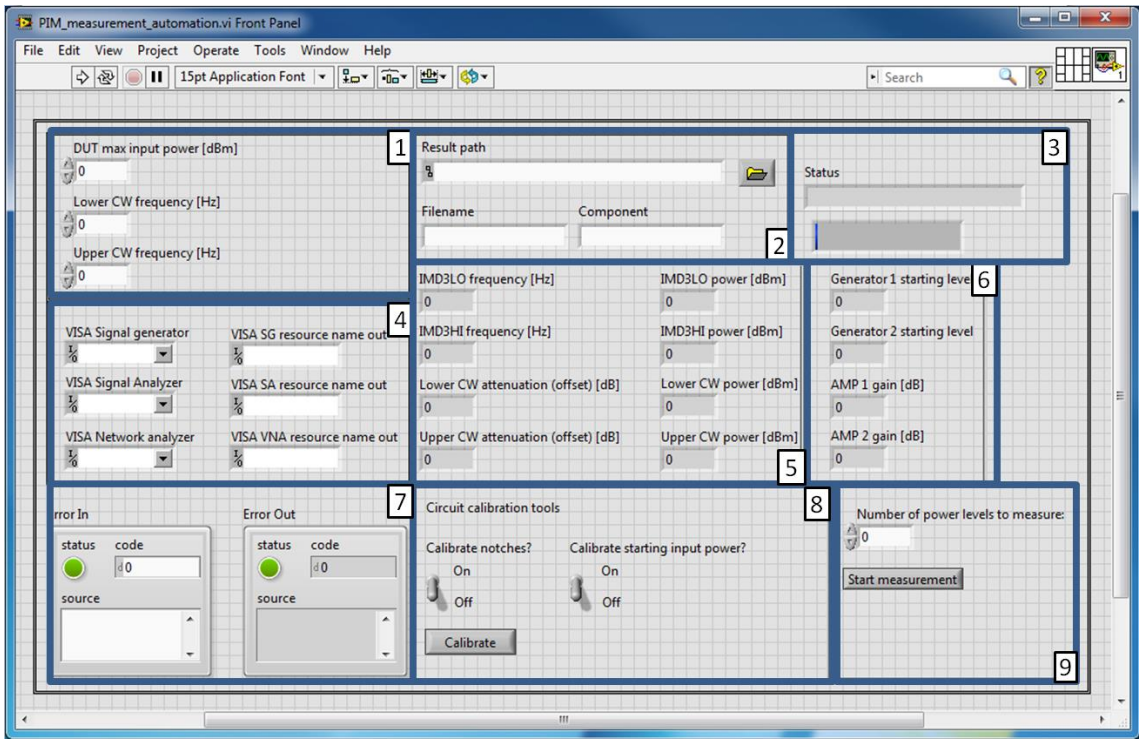

Picture 13. User interface of a passive intermodulation measurement and analysis VI

Section 1 in picture 13 contains the measurement system parameters of a passive intermodulation measurement VI. A user must input a DUT maximum input power and the CW frequencies used.

Section 2 contains the controls for a result path and a file name. A component name is an optional input and if it is given, it is concatenated into a filename. This enables the user to have measurement data of multiple components with common parts in file names.

In section 3, user can view the status of the measurement. Section 4 contains VISA interface resource name definitions.

From section 5, the user can view results from the current measurement loop. Section 6 contains the calibration coefficients. Section 7 contains LabVIEW Error in and Error out- clusters. In section 8, calibration routines can be selected and started. Section 9 contains the setting for sweep power levels and the button to start measurement.

5.3 Block diagrams and functional description

The block diagram explained in this chapter is linked to controls and indicators seen in the user interface in picture 13 in chapter 5.2. The passive intermodulation measurement VI explained contains multiple sub-VIs for the calibration of a measurement circuit, the actual measurement and the measurement data logging.

5.3.1 Calibration software

A passive intermodulation measurement circuit contains multiple components. While most of the components attenuate an RF signal, amplifiers are used to gain necessary power levels at a DUT input. Since a circuit contains multiple attenuations and amplifiers, measuring all of them by hand as a calibration before the measurement of the component itself is not feasible. Thus, an automated calibration tool was needed.

The calibration can be started from the main user interface seen in picture 13, section 8. Calibration data is saved for the time the main VI is open, and several

components can be measured in series if used frequencies and maximum input power remain the same. Also, calibration data can be reviewed in the front panel from section 6 in picture 13.

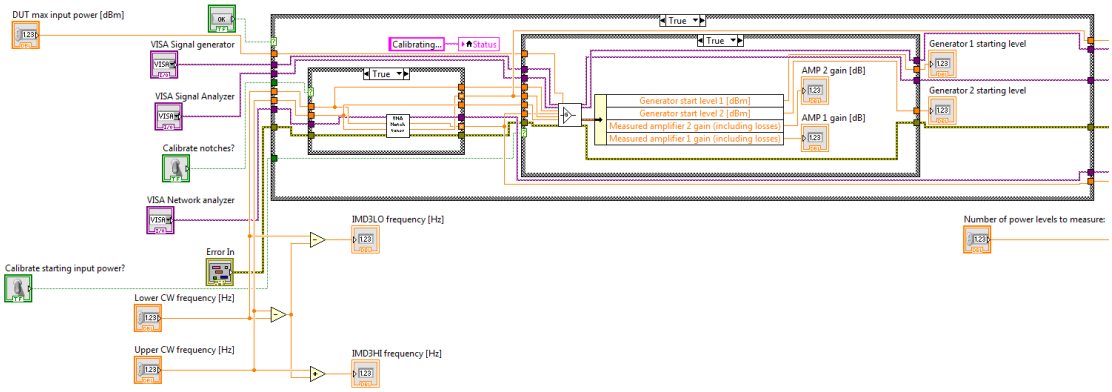

Picture 14. Block diagram of the calibration phase of a passive intermodulation measurement VI

Before starting calibration software, a user needs to input the maximum input power of the DUT, which can usually be seen in data provided by the manufacturer.

When a calibration routine is started, a dialog box shows informing the user to connect a tunable filter to a network analyzer. Then, a dialog box informs to perform the tuning:

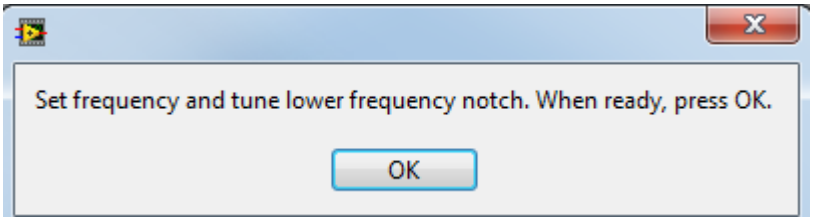

Picture 15. One of dialog boxes guiding the user during a calibration routine

When the filter is tuned, the user must press OK-button in a dialog box to continue. Then, automation software measures filter's the attenuation at a set fre-

quency. This data is then saved, and output to the main VI, where it is used as an offset to an measured power level. This operation is repeated for all filters needed.

The second calibration routine measures the gain of amplifiers used. This ensures that the maximum input power at DUT does not exceed the manufacturer's specifications. The gain calibration routine also takes losses in a circuit before DUT into note, removing the need for additional loss calibration. A filter calibration routine needs to be run before calibrating the gain.

After the calibration, the measured calibration coefficients can be reviewed from the UI.

5.3.2 Instrument control

For instrument control, several sub-VIs were developed. These include the control VIs of:

- Signal generator, explained in chapter 5.3.2.1
- Spectrum analyzer, explained in chapter 5.3.2.2
- Network analyzer , explained in chapter 5.3.2.3

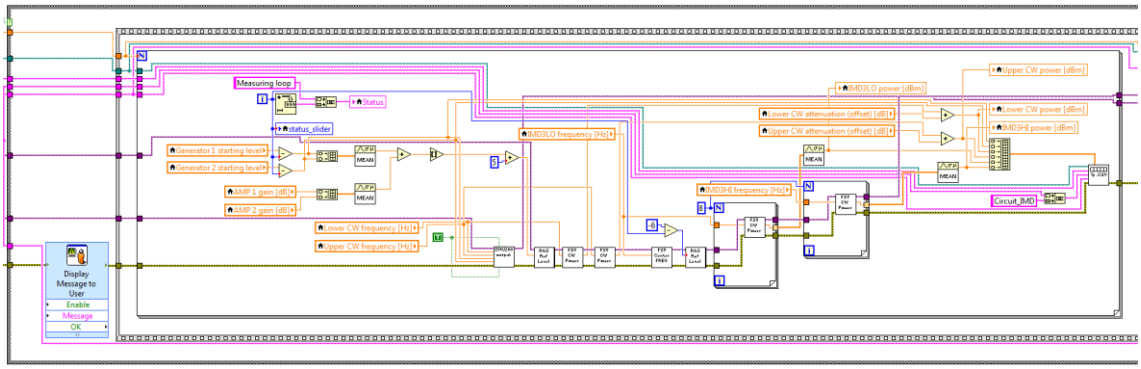

Picture 16. Block diagram of the measurement phase of the passive intermodulation measurement VI

In picture 16, several sub-VIs can be seen. These VIs are explained in the following chapters 5.3.2.1, 5.3.2.2 and 5.3.2.3.

5.3.2.1 Signal generator control VI

A signal generator control sub-VI can be used to set an output power, a frequency and to activate an RF output in the used generator:

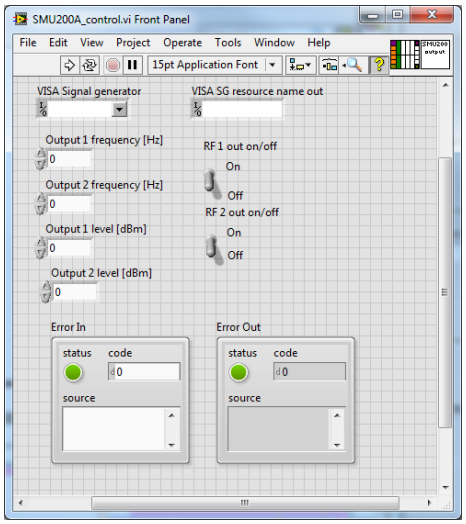

Picture 17. Front panel of the signal generator control VI

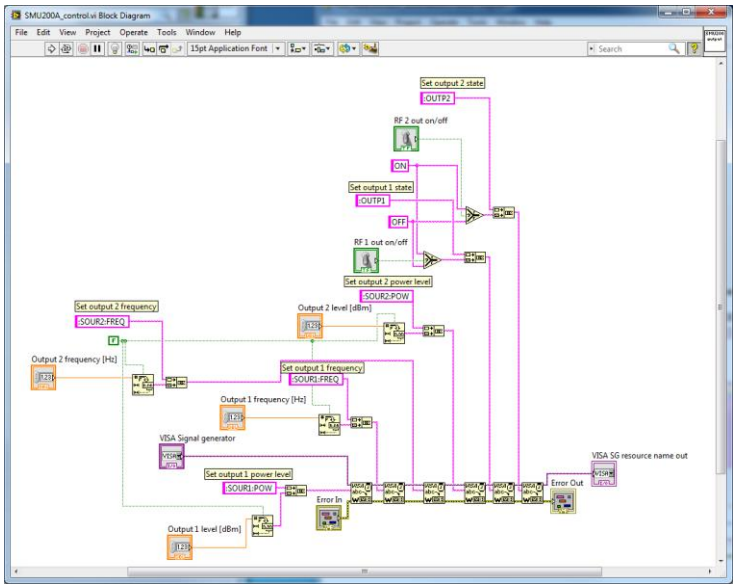

Picture 18. Block diagram of the signal generator control VI

The signal generator VI controls the Rohde & Schwarz SMU200A signal generator used. The signal generator has two individual outputs which both are con-

trolled with the same VI. The VI can be used to set the power level and frequency of the generator output and to switch the output state on and off.

The power level is set by converting the entered floating point value into ASCII string. The result is then concatenated into the SCPI command ":SOURn:POW", where n is the number of controlled output. For the generator to read the command correctly there must be a space character between the command and the parameter. Also, the regional settings of the controller PC must be set so comma is the decimal point.

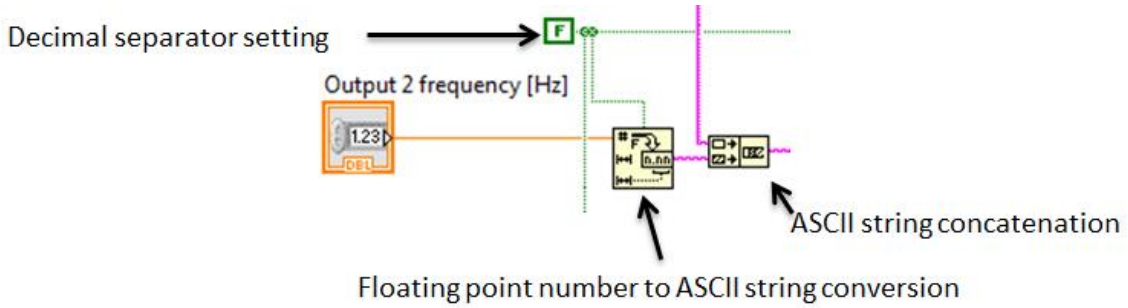

Picture 19. Decimal separator setting, a number to a string conversion and concatenation operations

If dot is used as a separator, the false constant in picture 19 must be changed into a true constant. This constant sets the use system decimal point-parameter in the fractional number to string-operation.

Setting the frequency is also done by converting the floating-point value entered into VI to an ASCII string format, and concatenating the result string into an SCPI command ":SOURn:FREQ ", where n is the number of the controlled output . As with the power setting, there must be a space character in the command. Also, the same regional setting constant that is used in a power setting is used in a frequency setting.

The on/off-state of the output is defined by the two boolean switches in the UI. Depending on the switch state, either an ON or OFF ASCII string is concatenated into SCPI command ":OUTPn", where n is the number of the controlled output. This is done by using the select operation. The select operation connects

one of two inputs into one output depending on the setting of the third input, which is either boolean true or false.

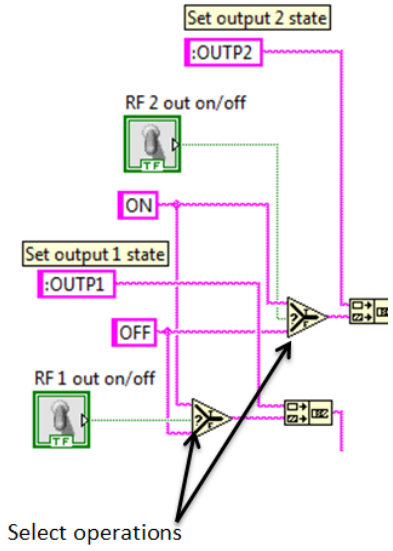

Picture 20. The select operations

All SCPI commands needed were found in the instrument's operating manual (30).

5.3.2.2 Spectrum analyser VIs

Spectrum analyzer VIs are used to read marker data, set reference level, frequency span and center frequency.

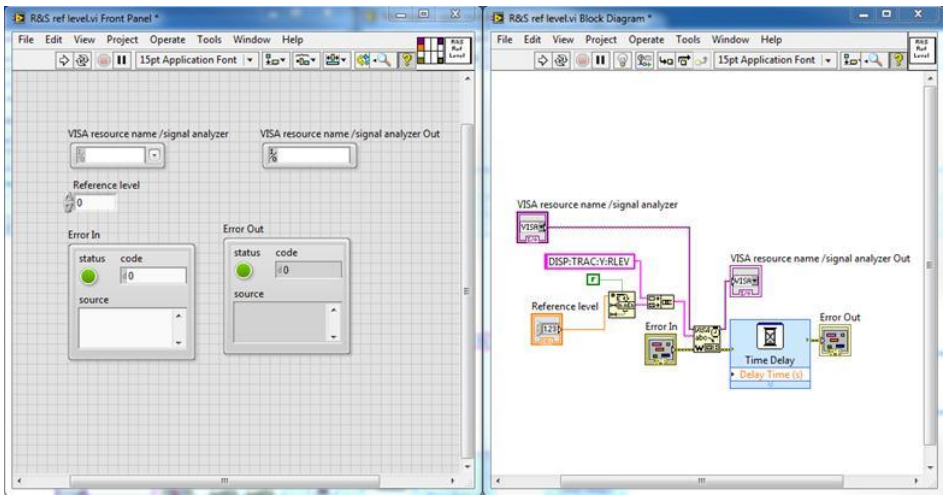

Picture 21. Front panel and a block diagram of a reference level setting VI

The VI in picture 21 sets a reference level of the FSV spectrum analyzer. This is done by concatenating the input reference level value into an SCPI command “DISP:TRAC:Y:RLEV “. The resulting string is then sent via VISA interface into the instrument. The VI contains a delay, thus the instrument can execute next sweep before the next VI is allowed to run.

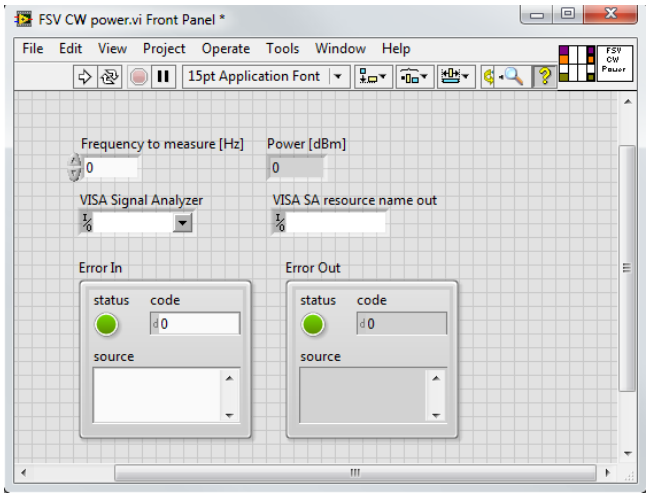

Picture 22. Front panel of a CW power measurement VI

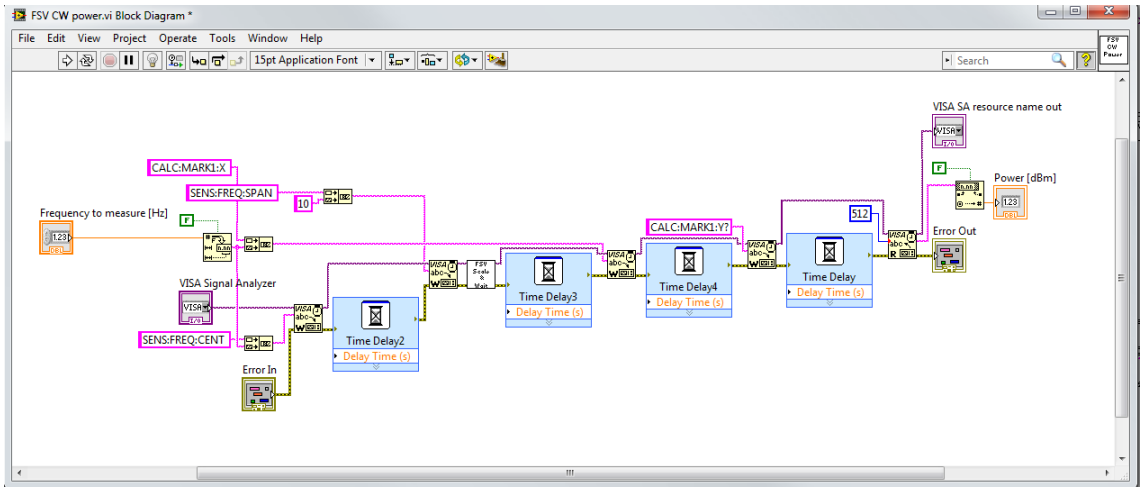

Picture 23. Block diagram of a CW power measurement VI

The VI seen in pictures 22 and 23 measures the power of a CW signal. The VI sets the frequency span of the analyzer into a narrow setting, 10 Hz. This ena-

bles an accurate CW power measurement. The frequency span of an FSV spectrum analyzer is set with an SCPI command “SENS:FREQ:SPAN nn”, where nn is the desired frequency span. The VI is input the frequency of the CW signal and it sets the center frequency of the analyzer into this value. After the center frequency, marker x-location and span are set, an auto scaling function is performed in the analyzer, followed by an “*OPC?” query. Thus, it is certain that the sweep is complete before reading the marker data Marker data is read by using an SCPI query “CALC:MARKn:Y?”, where n is the number of the marker.

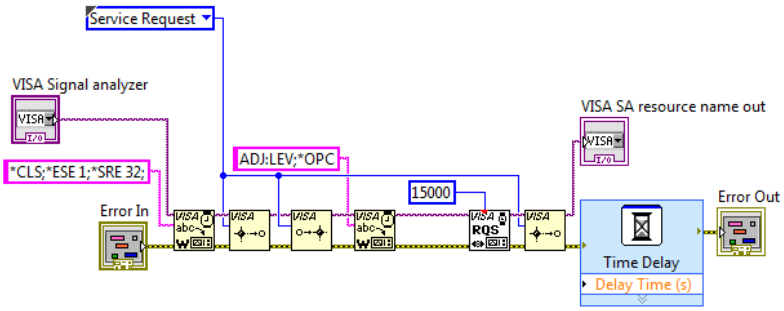

Picture 24. Block diagram of the VI performing an auto scaling function and an OPC query

All SCPI commands used were documented in the FSV spectrum analyzer’s operating manual (28).

5.3.2.3 Network analyser VI

A network analyzer control VI is used in a calibration phase. It is used to read markers during the filter tuning. These results are used as offsets in a spectrum analyzer.

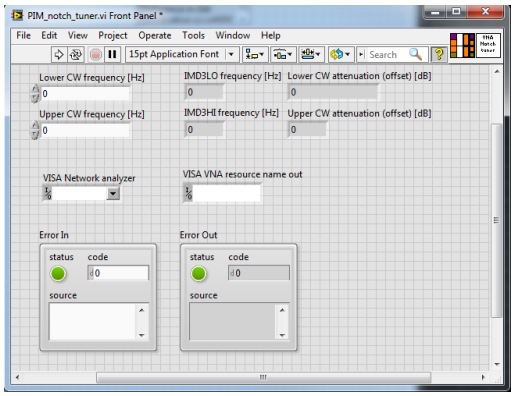

Picture 25. Front panel of the network analyzer VI

A block diagram of this VI is extensive and thus it is seen in appendix 1.

The VI is given the frequencies of the used CW signals as inputs. The IM3 frequencies are then calculated. The VI sets the center frequency of the network analyzer into the first CW frequency given and displays a dialog box for the user. Then, the user can tune the filter and save the tuned filter response by pressing an OK-button in a dialog box. This is repeated for total of four filters, two for the CW signals and two for the circuit-produced IMD3 signals. The response value from CW filters is then used as a calibration offset in a CW power measurement. As with the signal generator and spectrum analyzer, the needed SCPI commands were documented in the instruments operating manual (2).

5.3.3 Data logging

The data logging in this example is done by writing measurement results of each measurement loop into a comma separated value (CSV) file. This saved data can then be edited and processed by, for example, Microsoft Excel or MATLAB. The format of the CSV is the following:

ROW1COLUMN1; ROW1COLUMN2;…; ROW1COLUMNn<cr>
ROW2COLUMN1; ROW2COLUMN2;…; ROW2COLUMNn<cr>

Each row is followed by a carriage return-character. When using Finnish regional settings, the ";"-character marks the column separation. In for example US regional settings, this character is comma.

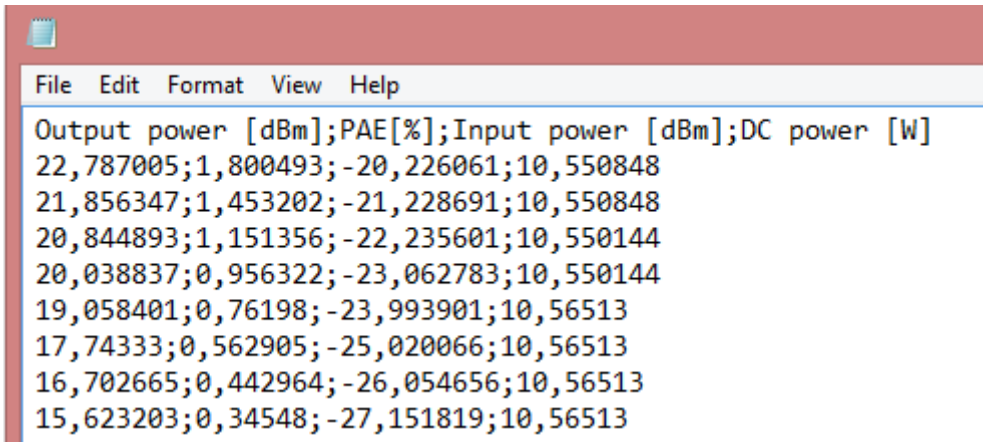

Picture 26. An example .CSV-file opened in a text editor

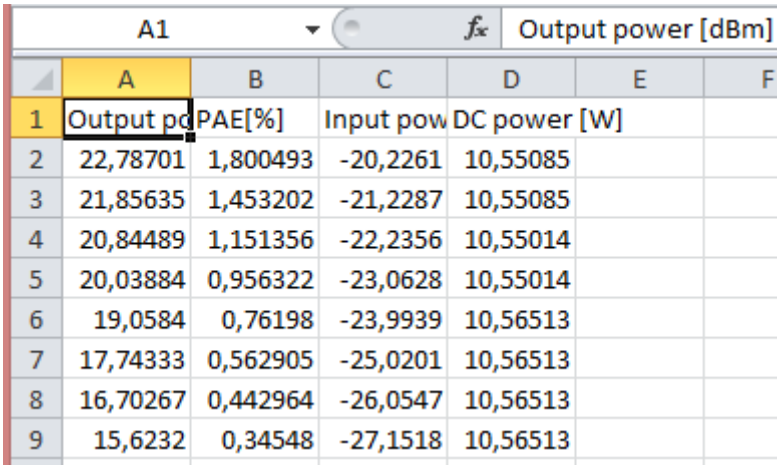

Picture 27. Example .CSV-file in Excel

In pictures 26 and 27, a .CSV-file is seen in both Notepad and Excel.

In MATLAB, data contained in a CSV file can be imported into variables. Importing is done using a GUI import tool, which can be opened either from menu or by using MATLAB command "uiimport".

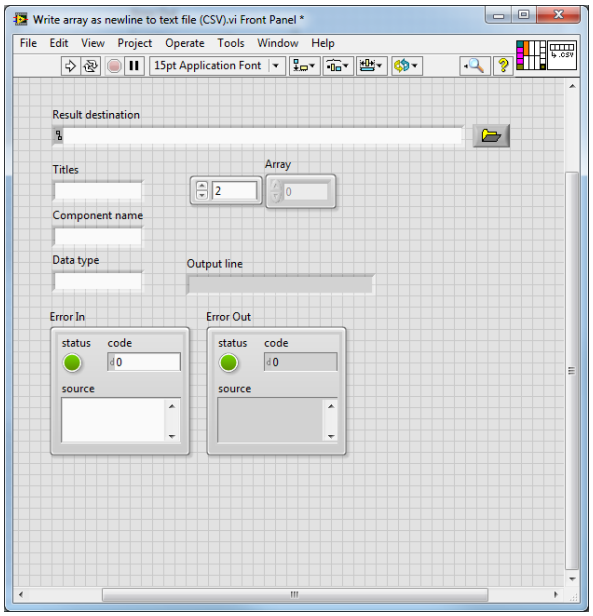

Picture 28. Front panel of the data logging VI

The VI used for the data logging has inputs for the array of results, destination folder, .CSV titles, component name and data type. The component name and data type are concatenated and they form the file name.

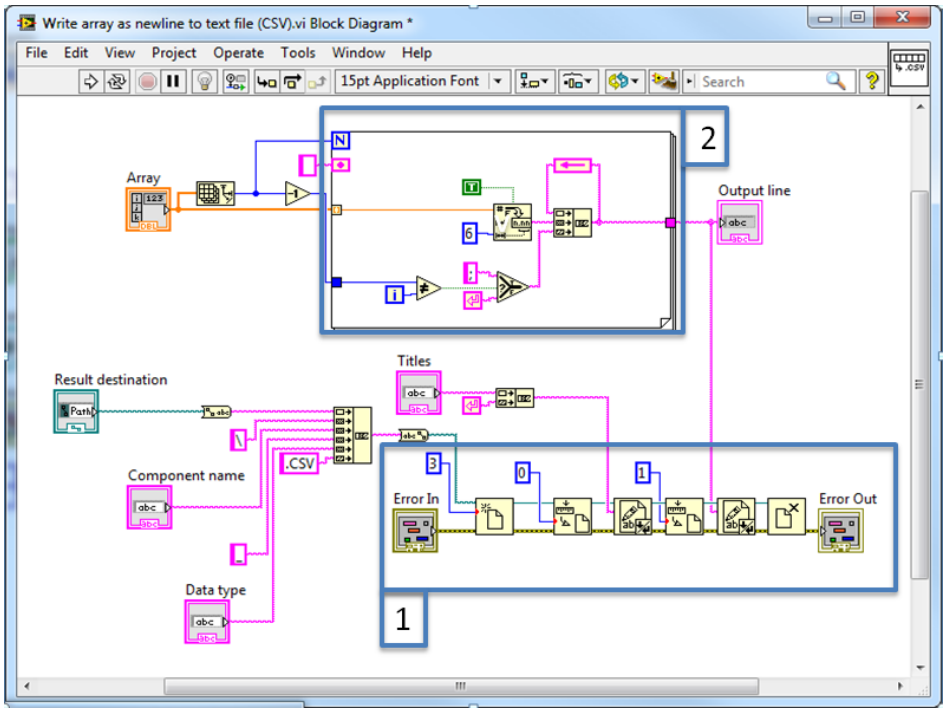

Picture 29. Block diagram of the data logging VI. In section 1, the file operations are seen. In section 2, the numerical array is parsed into a string in a .CSV format

In the block diagram seen in picture 29, the VI first opens a file. If the file does not exist, it is generated. If the file exists, data is appended into the end of the file as a new row.

The input array is converted into a string format cell-by-cell. A separator character ";" is added between the data cells. When the loop reaches the end of the array, a carriage return character is concatenated into the string.

5.4 Example results

As an example, PIM of an RF combiner was measured.

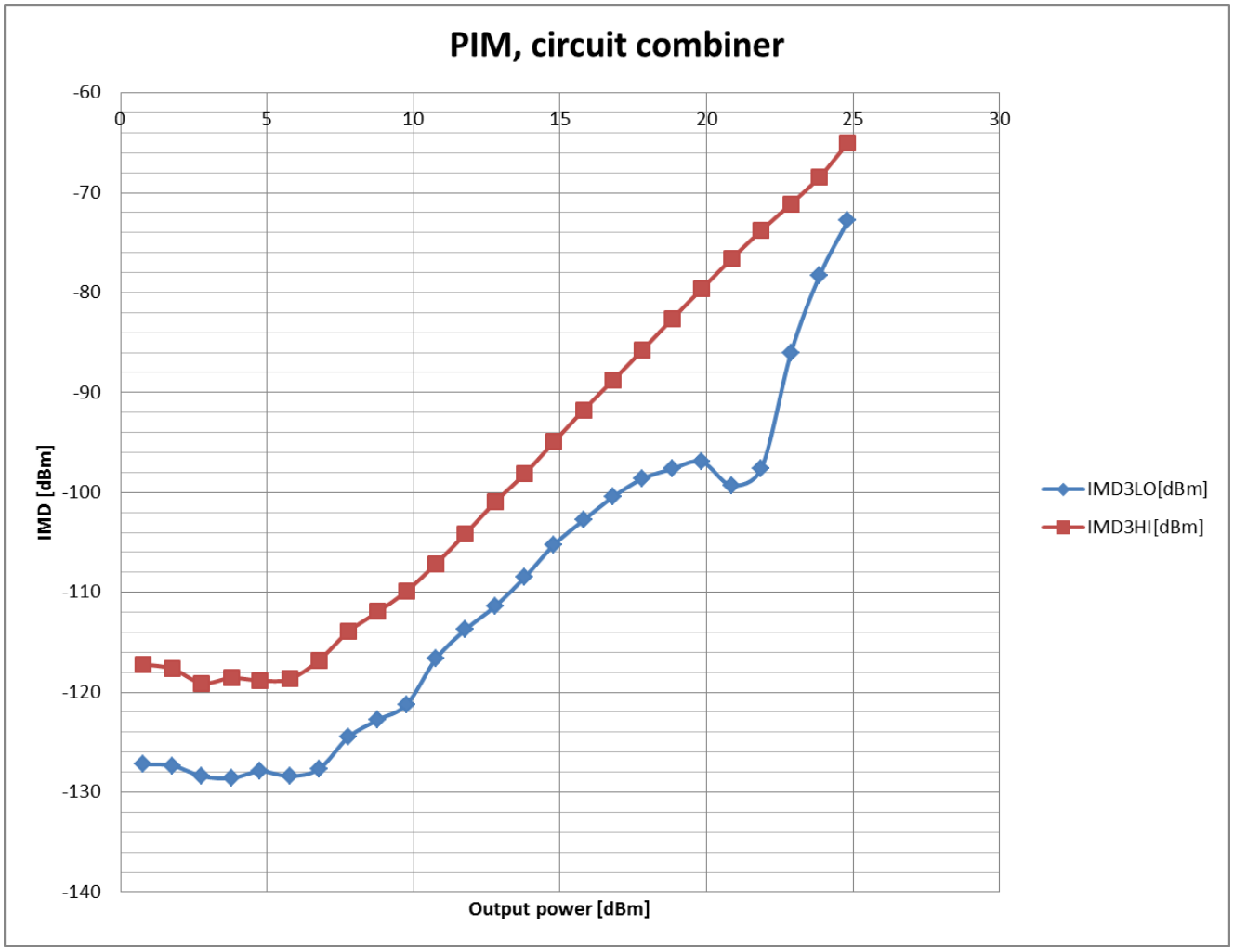

Figure 28. PIM measurement results from a circuit combiner

From figure 28, it can be seen that PIM does not necessarily follow the 3 dB IMD rise/1 dB input power rise rule. This measurement was repeated and the same results were obtained. As a conclusion, it can be stated that this RF combiner cannot be used in PIM measurement circuits with power levels exceeding +20 dBm if no additional IMD3 filtering is used and 100 dB is set as the limit of a circuit dynamic range.

5.5 Problems during development

The only problem during the PIM measurement automation development was the lack of high quality RF combiner for the circuit. Using the first RF combiner obtained, the dynamic range was only 70 dB, caused by a high PIM production of the RF combiner. After a higher quality combiner was obtained, a dynamic range of 105 dB was achieved at the highest power level used. The dynamic range could be extended further by using more resonator filters in the input of the DUT to remove circuit-based IMD products or by using a higher quality RF combiner.

5.6 Conclusions

The measurement results obtained using the automation were compared internally and it was found that they were accurate if the calibration was done using precision. The performance of filters used and that of the RF combiner in a circuit was the main limiting factor in accuracy if the calibration was valid. Due to the nature of resonator filters, the frequencies used had effect on the maximum possible attenuation of the tunable filter. Thus, the measurement frequencies had a direct effect on the dynamic range and hence the accuracy.

6 AUTOMATION SOFTWARE FOR POWER AMPLIFIER MEASUREMENTS

A power amplifier measurement automation was chosen as a second example. The automation measures a power amplifier's linearity and efficiency in user defined ambient temperatures and in at user defined input power levels. Vötsch VT 4004 environmental chamber is used to maintain the temperature. The measurements are done using a Fluke multimeter for voltage and current, an Agilent N1914A power meter for input power and a Rohde & Schwartz FSV13 signal analyzer for both output power and linearity. Additionally, a programmable attenuator is used to maintain a constant mixer level at the signal analyzer for a maximum accuracy and dynamic range. This mixer level is defined to be -17 dBm in FSV analyzers manual (28). The system contains two devices under test; the first one is the TX module used to generate signals and the second one is the amplifier.

In addition to the amplifier evaluation, the system is used to test different radio algorithms. This is done by using MATLAB to process the transmitted signal before it is loaded to the TX module. MATLAB processing is integrated to the automation software.

6.1 Measurement system

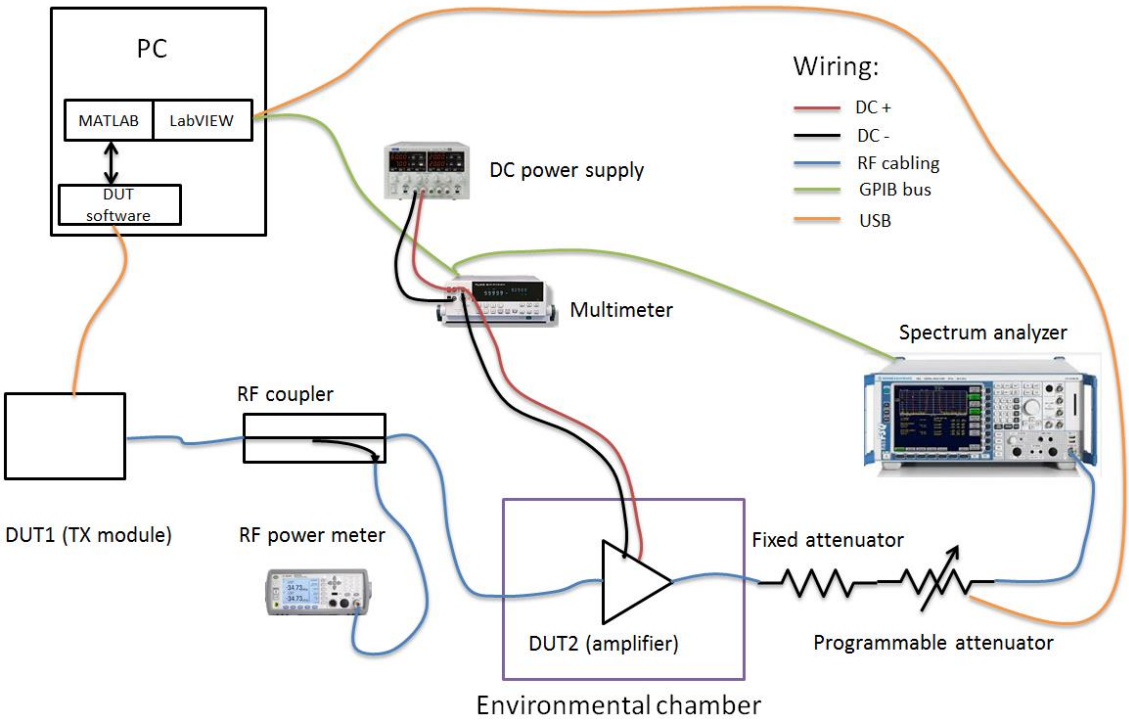

Picture 30. Illustration of the measurement system used (5)

The measurement system used for power amplifier measurements consists of multiple components:

- A TX module, which is used as a signal source. At the same time, the TX module performance is measured.
- An RF coupler, which is used to measure the input power in conjunction with the power meter
- An RF power meter, which is used to measure input power of the amplifier. Losses are calibrated as in the example system in chapter 4.2, figure 20. The calibration offset is defined as in formula 23
- The amplifier under measurement
- A DC power supply for the amplifier
- A multimeter, which is used to measure DC voltage and current. The multimeter used was capable of concurrently measuring both quantities

- A fixed attenuator for lowering the programmable attenuator input power level. The problem related to input power is explained in chapter 6.4
- A programmable attenuator to maintain constant spectrum analyzer mixer input power throughout the measurement power sweep
- A spectrum analyzer with ACLR measurement option for easy wideband signal measurement
- A controlling PC with LabVIEW, MATLAB and TX module control software
- An environmental chamber to test the amplifier in different ambient temperatures

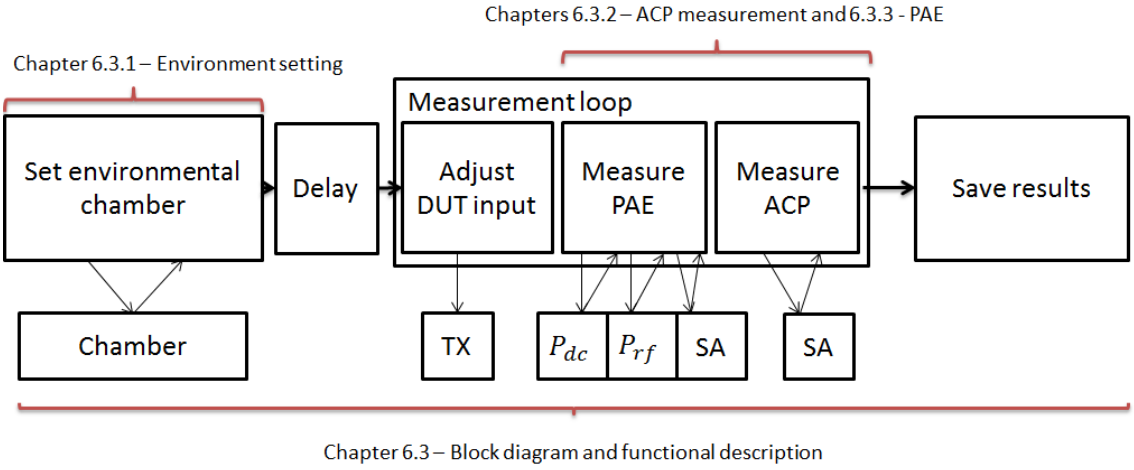

Picture 31.Block diagram of the TX measurement automation software

6.2 User interface of power amplifier measurement automation software

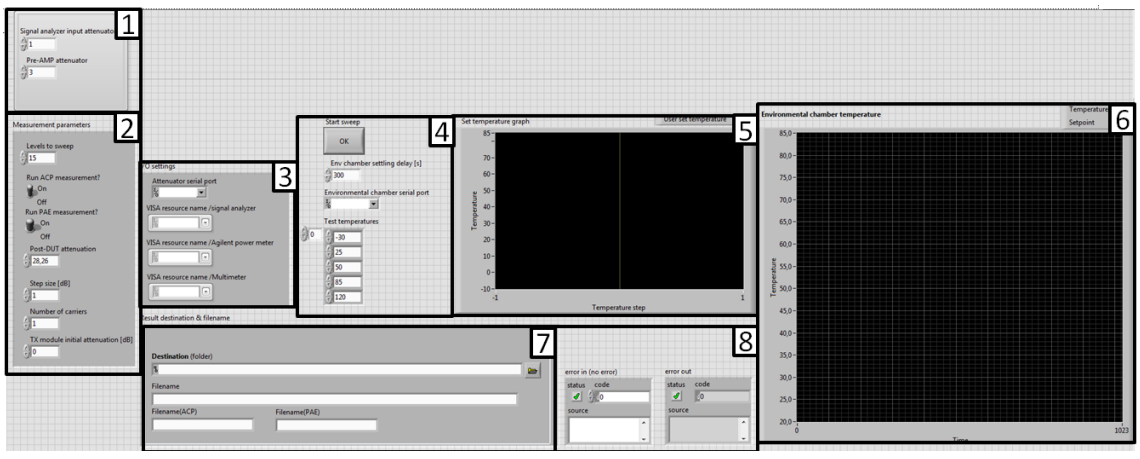

Picture 32. User interface of the TX measurement automation software

The user interface of the power amplifier measurement automation seen in picture 32 contains VISA resource name controls and measurement parameters needed. In section 1, the user can set the I/O settings of a programmable attenuator in spectrum analyzer input. Another attenuator can optionally be used to control input power, if a TX module is not used. The attenuator used had four I/O:s.

In section 2, the user can define the power levels to sweep, post-DUT attenuation for calibration offset, step size, number of carriers and the TX module initial attenuation level. Also, the user can choose if ACP and PAE measurements are executed.

Section 3 contains the VISA interface settings. The attenuator is connected through a serial port, thus a COM port must be chosen. Section 4 contains a measurement execution button, the temperature parameters and the serial port used for communication with the environmental chamber. The temperatures are input in the array in ˚C. In addition, an adjustable delay can be set if needed. Section 5 contains a graph illustrating the temperatures the user has input. In section 6, a graph showing the user set temperature and actual temperature in an environmental chamber is seen.

Section 7 contains the folder selection for results and file name inputs. LabVIEW Error In and Error Out clusters are seen in section 8.

6.3 Block diagram and a functional description

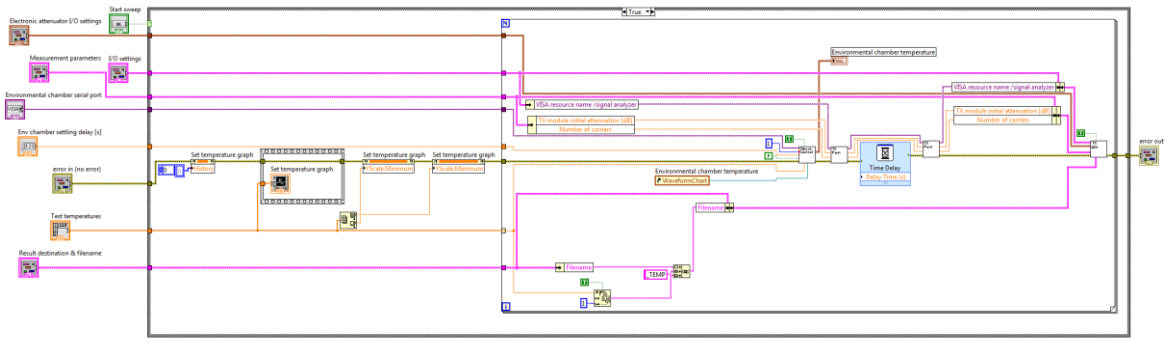

Picture 33. Block diagram of the main VI of the TX measurement automation

6.3.1 Environment setting

A Vötsch VT 4004 environmental chamber used had a serial input for external control. No LabVIEW drivers were found for the chamber model precisely, but drivers found for Vötsch VT 4002 were found suitable. A minor editing was required to change from the use of fixedly defined COM ports to a more flexible VISA interface. Since the development of this VI was not part of the thesis work, the block diagram is not explained.

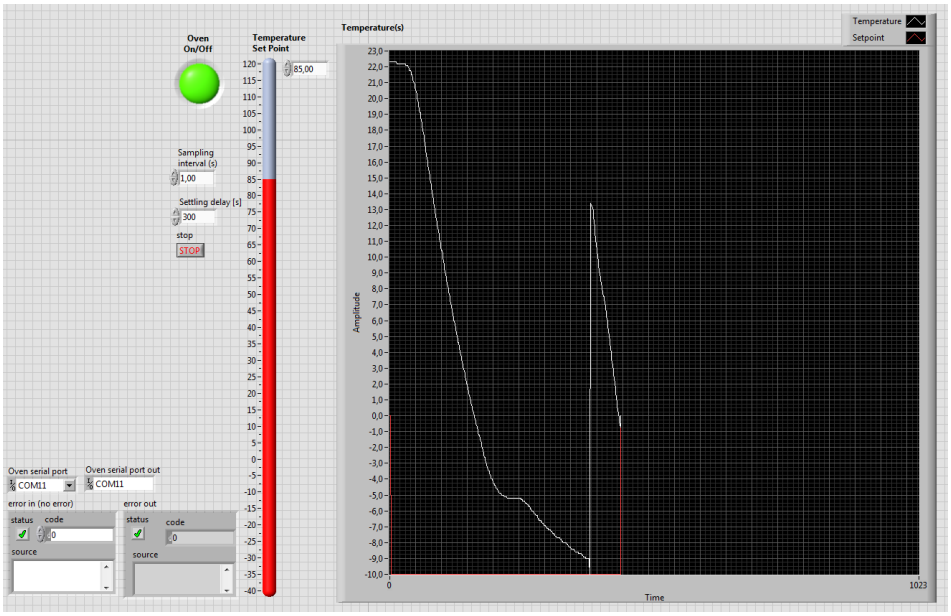

Picture 34. Front panel of the environmental chamber control VI

The VI gets the wanted temperature setting as input and outputs the current temperature. Additionally, a user-definable delay can be set to ensure that the temperature of DUT is settled.

6.3.2 ACP measurement

The Rohde & Schwartz FSV Spectrum analyzer used in the measurements had an option for wideband ACP measurements. Thus, automating the adjacent channel power measurement only required a single SCPI query to transfer the results into a controller.

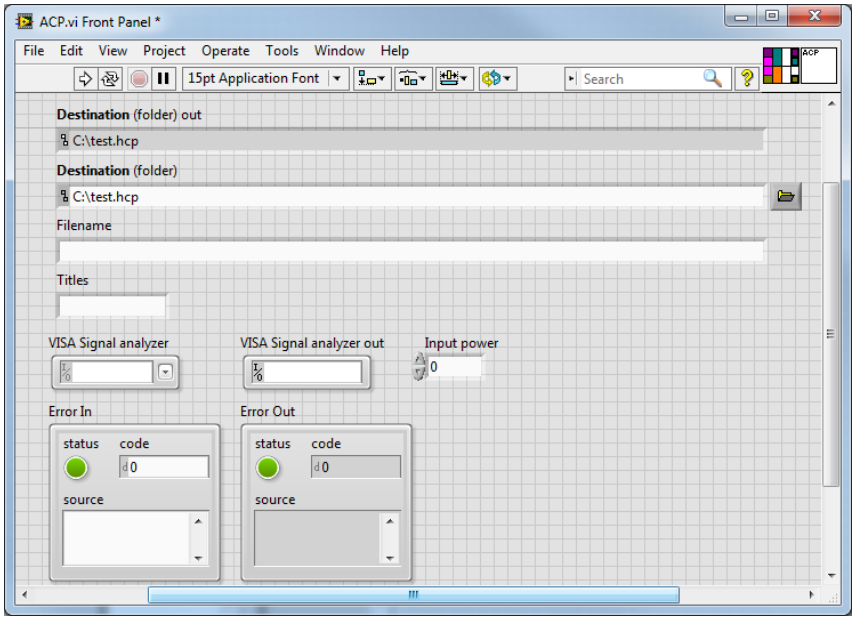

Picture 35. Front panel of the ACP measurement VI

The ACP measurement VI seen in pictures 35 and 36 has inputs for a result destination, file name, .CSV titles and input power. The input power is added into the first index of the result array.

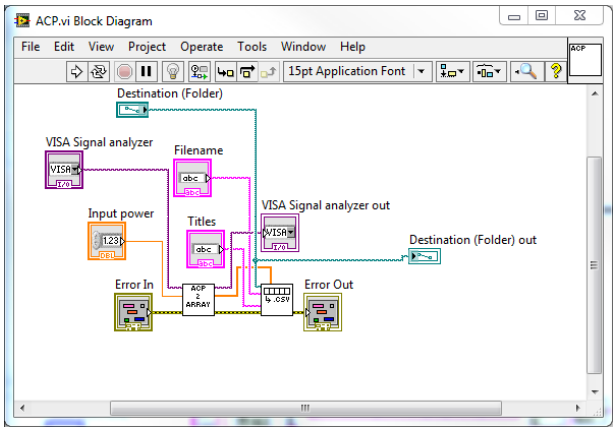

Picture 36. Block diagram of the ACP measurement VI

The VI uses two sub-VIs; the first one queries the ACP measurement results from the instrument and parses them into a numerical array and the second one writes this array into a text file. The sub-VI used for saving the results into a file is the same as in chapter 5.3.3.

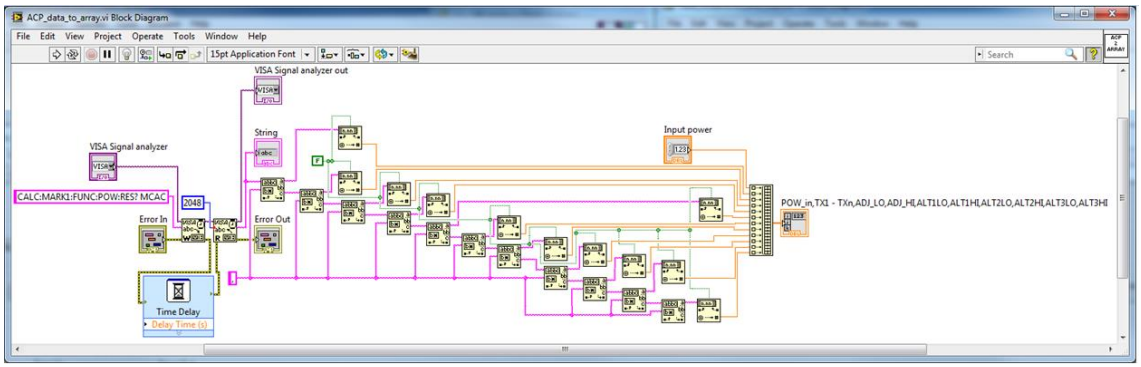

Picture 37. Block diagram the ACP result query VI

As a result to the SCPI query “CALC:MARK1:FUNC:POW:RES? MCAC” a string containing the measurement results is received. The results are in the following format:

TX1,TX2,…,TXn,TX_TOTAL,ADJ1LO,ADJ1HI,ALT1LO,ALT1HI,…,ALTmHI

where n is defined by the number of carriers measured and m is defined by the measured ACP channel pairs. This string is then parsed into a numerical array. A total of 11 results can be parsed into a numerical array using this VI.

6.3.3 PAE measurement

A power added efficiency is measured according to the specifications explained in chapter 3.2. First, a spectrum analyser is used to measure the output power of DUT. Then, a multimeter is used to measure voltage and current. Using Ohm’s law, a DC power can then be calculated:

FORMULA 25. Ohm’s Law

$$P = UI$$

where

P = DC power in watts,

U = voltage in volts and

I = current in amperes.

The input power of the DUT is then measured with an RF power meter. From these results, PAE is calculated using the formula 16 in chapter 3.2.

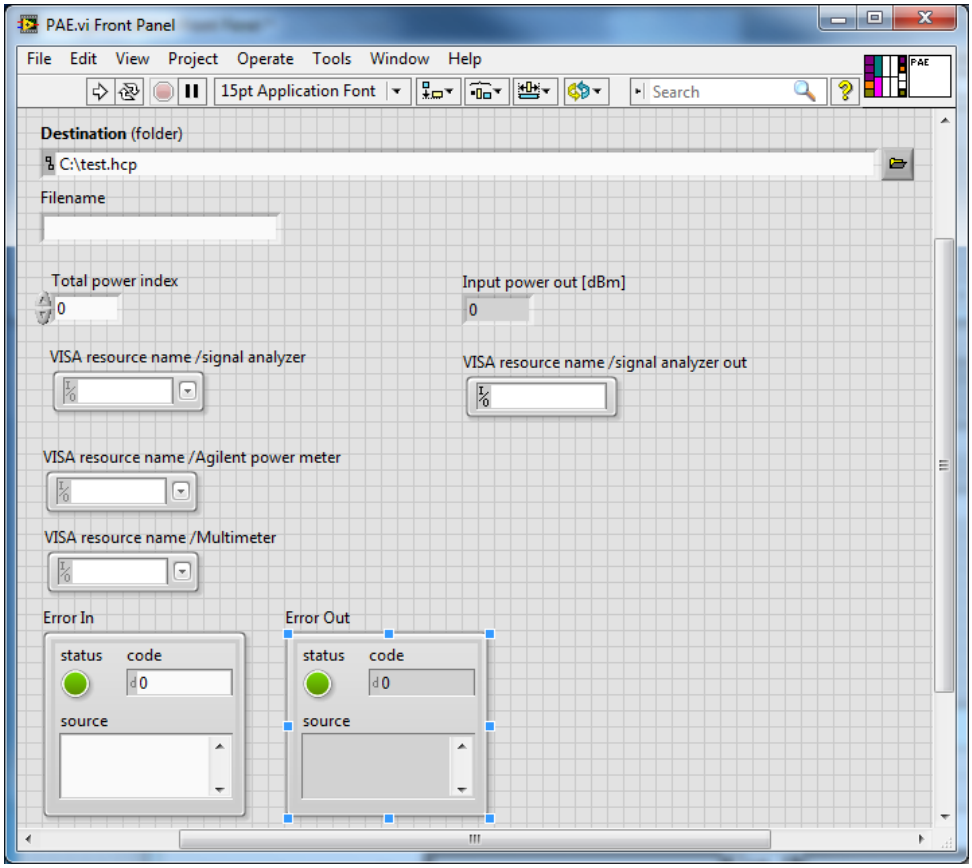

Picture 38. Front panel of the PAE measurement VI

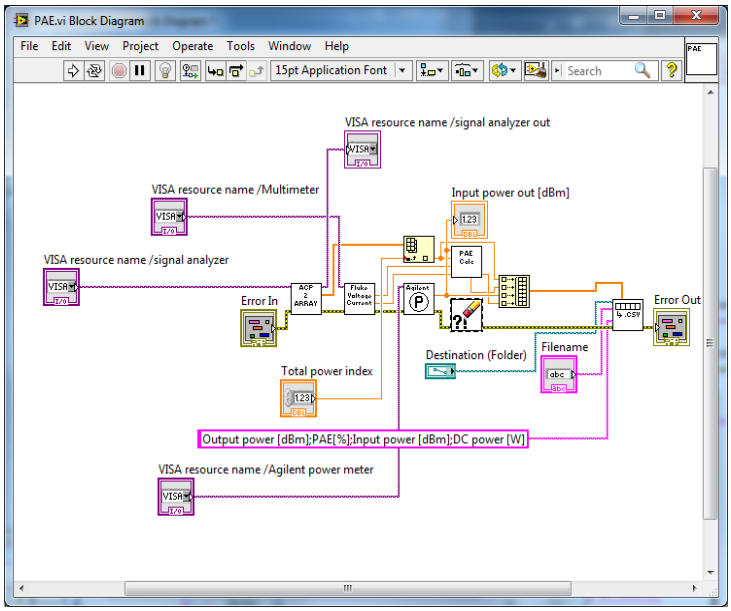

Picture 39. Block diagram of the PAE measurement VI

As seen in picture 39, the PAE measurement VI uses six sub-VIs to measure the results. First, the output power of DUT is measured with the spectrum analyzer. This is done by using the ACP measurement sub-VI. For voltage and current, a multimeter reading sub-VI is used:

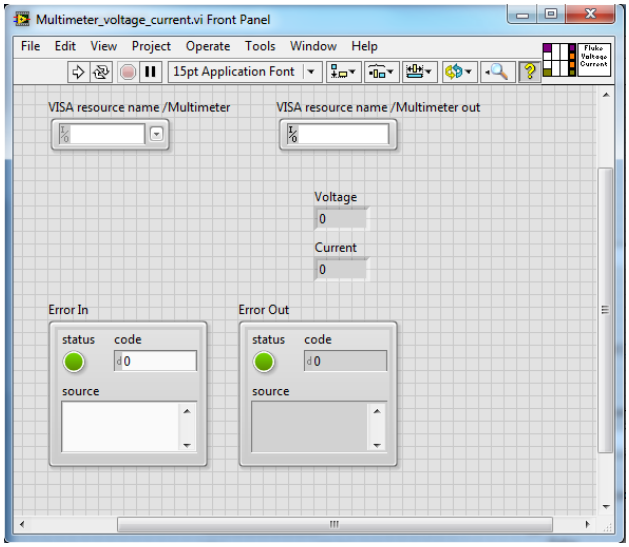

Picture 40. Front panel of the Multimeter VI

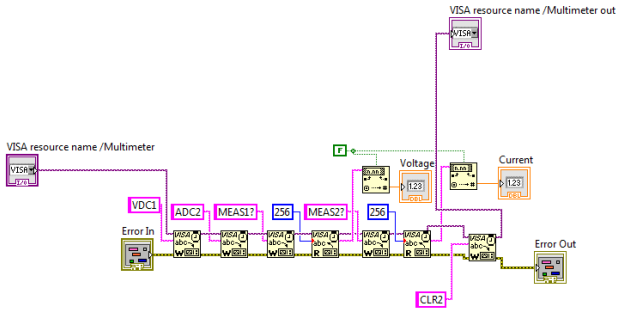

Picture 41. Block diagram of the multimeter VI

The used multimeter could measure both voltage and current simultaneously in a two-channel mode. The first channel is used to measure voltage using an SCPI command “VDC1”. The second channel is set to current measurement by an SCPI command “ADC2”. Then, the results are queried with commands “MEAS1?” and “MEAS2?”. The results of these queries are then converted to a numerical format. A “CLR2” SCPI command is used to a stop two-channel measurement at the end of the measurement, due to a loud clicking sound the meter produces in a two-channel mode.

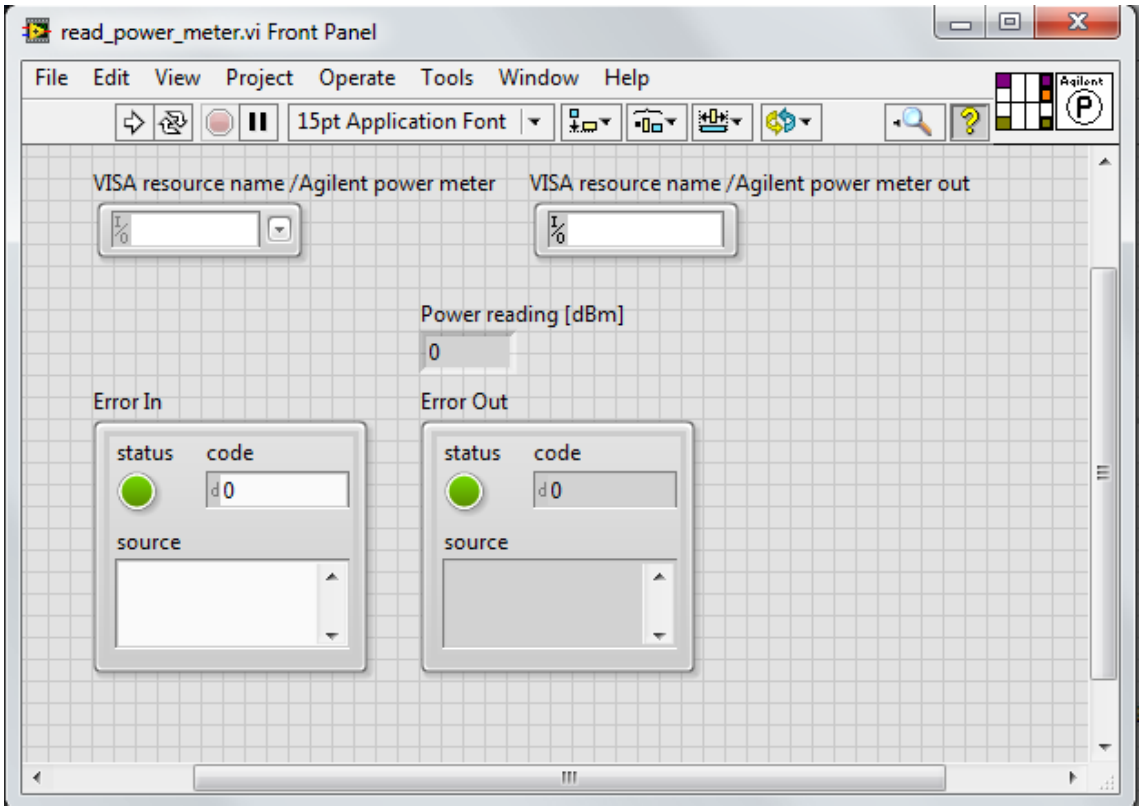

Picture 42. Front panel of the power meter VI

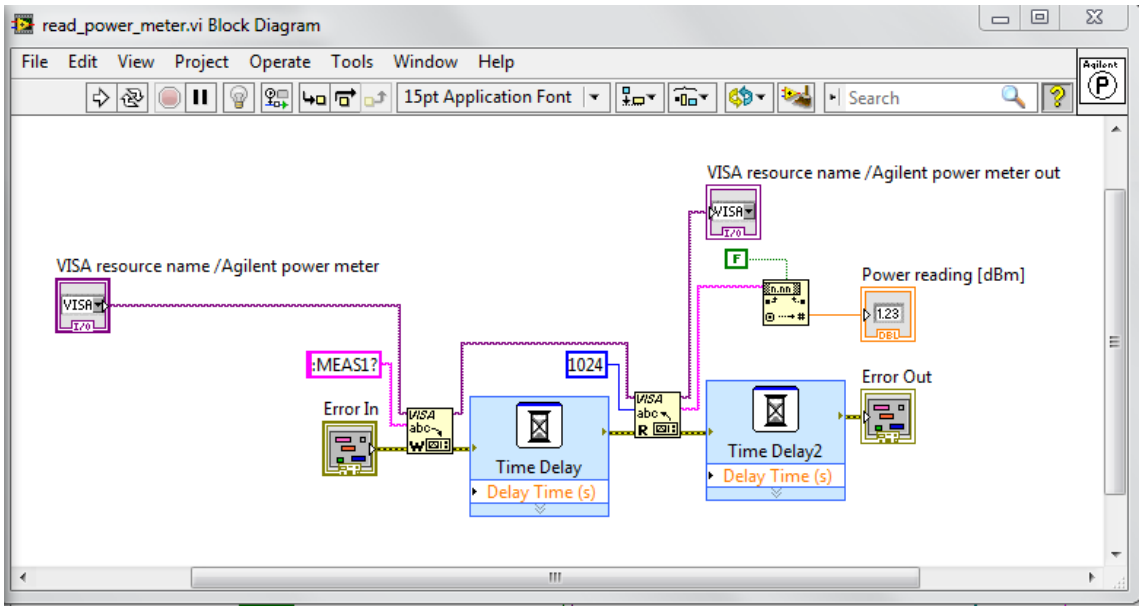

Picture 43. Block diagram of the power meter VI

After the voltage and current measurement, the power meter is used to measure the DUT input power. A single SCPI query ":MEAS1?" measures and returns the result power of channel 1 in power meter. It was noted during the development that power meter sometimes returns an error even if the result is acceptable. Thus, a remove error-VI was added to circumvent issues with the error.

After all quantities needed are measured, PAE is calculated using a sub-VI.

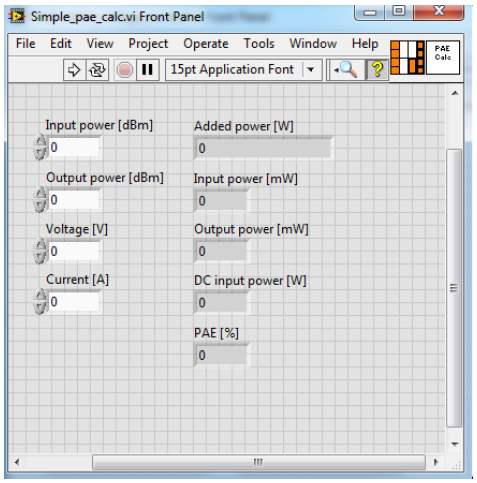

Picture 44. Front panel of the PAE calculation VI

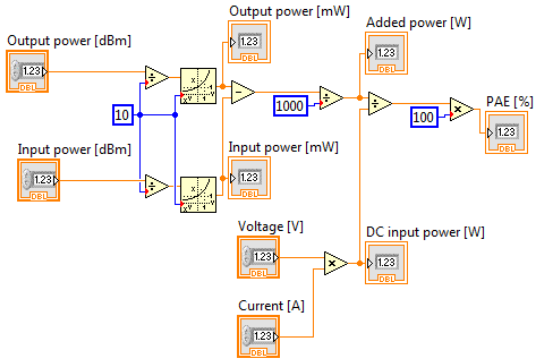

Picture 45. Block diagram of the PAE calculation VI

The sub-VI converts the power readings to Watts and subtracts the input power. Then, the DC power is calculated using Ohm's law, seen in formula 25, and the ratio of the DC power to the RF power is calculated. By multiplying this ratio by 100, a percentage PAE is obtained. This result is then written to a .CSV file using sub-VI explained in chapter 5.3.3.

6.3.4 Data logging

Data logging utilizes the same sub-VI that is explained in chapter 5.3.3. In addition, a screenshot is captured from the instrument in a .PNG format and transferred into the controller.

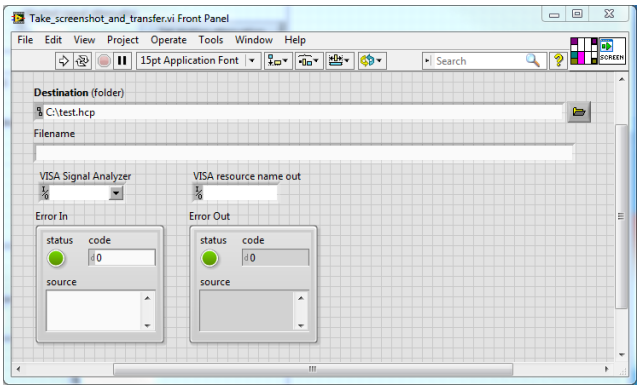

Picture 46. Front panel of the screenshot capturing and transferring VI

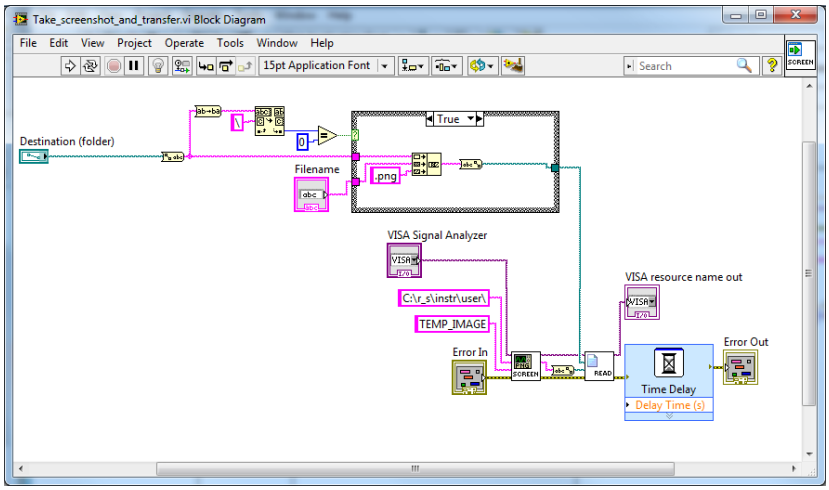

Picture 47. Block diagram of the screenshot capturing and transferring VI

The VI seen in pictures 46 and 47 first captures a screenshot in the instrument, saves it in a temporary file and then transfers it into the controlling PC to a user defined location. It consists of two sub-VIs. The first is used to capture the actual screenshot and save it to a temporary file in the instrument. The second sub-VI transfers this temporary file into the controller.

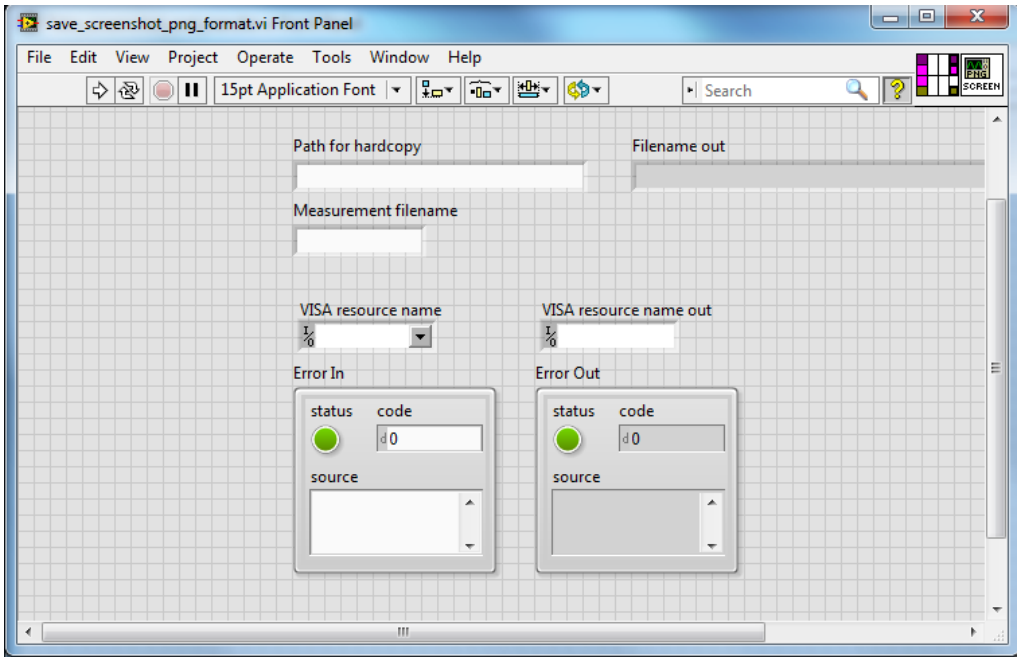

Picture 48. Front panel of the screenshot capturing VI

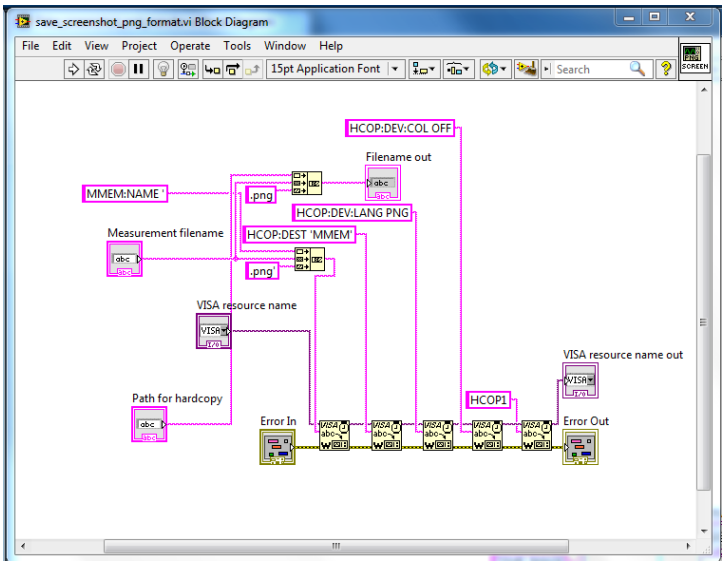

Picture 49. Block diagram of the screenshot capture VI

For the screen capture, the user must input a path and a filename for the temporary file. The format is defined to be a .PNG by SCPI command “HCOP:DEV:LANG PNG” and the display colors of the spectrum analyzer are set to black and white with an SCPI command “HCOP:DEV:COL OFF”. This is to ease reading and to save printer ink if the screenshot is to be printed to paper. Then, the capture is executed with an SCPI command “HCOP1”.

After the screenshot is captured into a temporary file in the instrument, it is transferred into the controller. This is done using a file transfer VI found in the Rohde & Schwarz FSV LabVIEW driver package. An example screenshot can be seen in chapter 3.1, picture 1.

6.4 Problems during development

There were many difficulties during the development. The first problem was with the MATLAB integration. It was caused by old version of a function that had same file name as a newer version. This caused the automation to get different results than those obtained manually. The problem was with the setting of the working folder in MATLAB Script Node used to integrate MATLAB functions into LabVIEW.

The second problem was a lower dynamic range when less input power was fed into the amplifier. The cause was found to be the noise generated by attenuator which was used in the input power setting. This was corrected by using the TX module for the signal power level control. Also, using a digital back off to set the signal power was deemed as a solution. However, if a digital back off was used the noise of the DAC would become dominant.

The third problem was the non-linearity content generated by a programmable attenuator in the measurement circuit. This was corrected by installing a fixed attenuator in the circuit before the programmable one. Installing the attenuator lowered the input power of the programmable one, removing the effects of non-linearity.

6.5 Conclusions

The power amplifier measurement automation became the most used one, due to the possibility to analyze radio algorithms. The results obtained were as accurate as those obtained using manual measurements. The measurement speed was significantly faster, since manually logging results from multiple instruments is relatively slow. Future work could include an automated reporting utility, which creates graphs and analysis results from the measurement results.

7 SUMMARY AND CONCLUSIONS

The main objective of this thesis was to automate five measurements defining the base performance of components used in radio transmitters and receivers. The quality and accuracy of the results were to be comparable to those gained by manual measurements. Studying the measurement environment was the secondary objective. Also, an explanation of basic radio architectures and components was to be given.

All planned measurements were automated. With automation the repeatability of the measurements was greatly improved and the risk of a human error was eliminated, as long as the calibrations were done with care. Measurement times were also improved greatly. Additionally, MATLAB functions for signal processing were integrated into the automation routines to ease the verification of them without the need of additional hardware. During the development of this thesis, dozens of different RF components were measured using automation.

In addition to the main objective, generic examples of RF transmitter and receiver architectures and components were included in this thesis. An overview of basic measurements and parameters was given with examples. A basic odd-order nonlinear model was created and explained.

Future work could include a development of automated reporting tools to ease work after the measurements. The speed of measurements could be improved by replacing the constant delays in software with “*OPC?”-queries. The change from GPIB to an LXI interface would also improve the capabilities of the system. LabVIEW supports the generation of TCP servers and this feature could be used to remotely control the setup.

The work on the thesis was often challenging and thus very rewarding. A precious insight on RF design, testing and automation programming was gained. Also, a lot was learned about signal processing, RF components and electronics in general. Last but not least, the skills in finding information in different sources were improved greatly.

REFERENCES

1. About 3GPP. 3GPP 2014. Date of retrieval 17.12.2013. Available at: http://www.3gpp.org/about-3gpp/about-3gpp

2. Agilent E5071C User manual. Date of retrieval 12.9.2013. Available at: http://www.home.agilent.com/agilent/editorial.jspx?cc=US&lc=eng&cke y=1659862&nid=-536902639.350794.00&id=1659862

3. Agilent PNA-X Application: Power-Added Efficiency (PAE). Agilent Technologies, Inc. 2007. Date of retrieval 22.10.2013. Available at: http://cp.literature.agilent.com/litweb/pdf/5989-7293EN.pdf

4. Application note - Intermodulation Distortion Measurements on Modern Spectrum Analyzers. Rohde & Schwarz 2012. Date of retrieval 2.3.2014. Available at: http://cdn.rohde-schwarz.com/dl_downloads/dl_application/application_notes/1ef79/1E F79_1E.pdf

5. Class B power amplifier. Circuitstoday.com article. Date of retrieval 5.11.2013. Available at: http://www.circuitstoday.com/class-b-power-amplifiers

6. Efficiency of microwave devices. Microwaves101.com article. Date of retrieval 21.1.2014. Available at: http://www.microwaves101.com/encyclopedia/efficiency.cfm

7. ETSI TS 125 101 V10.11.0 (2014-01) User Equipment (UE) radio transmission and reception (FDD) (3GPP TS 25.101 version 10.11.0 Release 10). Technical Specification. 2014. Sophia Antipolis Cedex: ETSI. Date of retrieval 15.11.2013. Available at: http://www.etsi.org/deliver/etsi_ts/125100_125199/125101/10.11.00_6 0/ts_125101v101100p.pdf

8. ETSI TS 136 104 V9.4.0 LTE Base station radio transmission and reception (3GPP TS 36.104 version 9.4.0 Release 9). Technical Specification. 2012. Sophia Antipolis Cedex: ETSI. Date of retrieval 10.12.2013. Available at: http://www.etsi.org/deliver/etsi_ts/136100_136199/136104/09.04.00_60/ts_136104v090400p.pdf

9. Facts & Figures. LM Ericsson 2014. Date of retrieval 8.3.2014. Available at: http://www.ericsson.com/thecompany/company_facts/facts_figures
10. Gain engineering note. EMPOWER RF SYSTEMS, Inc. Date of retrieval 8.12.2013. Available at: http://www.rf-amplifiers.com/index.php?topic=gain

11. González Gilda G. G. 2004. Measurements for modelling of wideband nonlinear power amplifiers for wireless communications. Helsinki: Helsinki University of Technology. Available at: http://signal.hut.fi/spit/publications/2004t2.pdf

12. GPIB Overview. The MathWorks, Inc. Date of retrieval 13.1.2014. Available at: http://www.mathworks.se/help/instrument/gpib-overview.html

13. History. LM Ericsson 2014. Date of retrieval 8.3.2014. Available at:http://www.ericsson.com/thecompany/company_facts/history

14. HetNet/Small Cells. 3GPP article. Date of retrieval 2.3.2014. Available at: http://www.3gpp.org/hetnet

15. Jantunen, Peter 2004. Modelling of Nonlinear Power Amplifiers for Wireless Communications. Helsinki: Helsinki University of Technology. Available at: http://signal.hut.fi/spit/publications/2004t1.pdf

16. LabVIEW VISA Tutorial. National Instruments. Date of retrieval 13.1.2014. Available at: https://www.ni.com/support/visa/vintro.pdf

17. Lämsä, Jukka 2014. Example measurement results, block diagrams, figures and pictures created for thesis work. Oulu: Oulu University of Applied Sciences.

18. Leinonen, M. 2013-2014. Various discussions with supervisor

19. MATLAB Script node reference. National Instruments 2012. Date of retrieval 18.10.2013. Available at: http://zone.ni.com/reference/en-XX/help/371361J-01/gmath/matlab_script_node/

20. Oppenheim Alan V. – Verghese George C. 2010. Signals, Systems and inference – Class Notes for 6.011: Introduction to Communication, Control and Signal Processing, Chapter 12. Massachusett: Massachusetts Institute of Technology

21. Poole, Ian. LTE Frequency Bands & Spectrum Allocations. Date of retrieval 19.11.2013. Available at: http://www.radio-electronics.com/info/cellulartelecomms/lte-long-term-evolution/lte-frequency-spectrum.php

22. Poole, Ian. QAM constellation comparison. Date of retrieval 16.3.2014. Available at: http://www.radio-electronics.com/info/rf-technology-design/pm-phase-modulation/8qam-16qam-32qam-64qam-128qam-256qam.php

23. Proakis, John G. – Manolakis, Dimitris G. 1996. Digital signal processing: principles, algorithms and applications. New Jersey: Prentice-Hall, Inc

24. Propagation characteristics. FCC tech article. Date of retrieval 10.12.2013. Available at: http://transition.fcc.gov/pshs/techtopics/techtopics17.html

25. Räisänen, Antti V. – Lehto, Arto 2003. Radio engineering for Wireless Communication and Sensor Applications. Norwood: Artech House

26. RF Power Values. Cisco Systems Inc. Date of retrieval 4.10.2013. Available at: http://www.cisco.com/c/en/us/support/docs/wireless-mobility/wireless-lan-wlan/23231-powervalues-23231.pdf

27. Rohde & Schwarz FSV Signal and Spectrum Analyzer LabVIEW driver package. Rohde & Schwarz 2013. Date of retrieval 12.9.2013. Available at: http://www.rohde-schwarz.com/en/driver/fsv/

28. Rohde & Schwarz FSV Signal and Spectrum Analyzer Operating Manual. Rohde & Schwarz 2013. Date of retrieval 12.9.2013. Available at: http://cdn.rohdeschwarz.com/dl_downloads/dl_common_library/dl_manuals/gb_1/f/fsv_1/archive_37/FSV_Operating_min.pdf

29. Rohde & Schwartz FSV Signal and Spectrum Analyzer Product Brochure. Rohde & Schwarz. Date of retrieval 23.1.2014. Available at: http://cdn.rohde-schwarz.com/dl_downloads/dl_common_library/dl_brochures_and_datasheets/pdf_1/FSV_bro_en_5214-0499-12_v1000.pdf

30. Rohde & Schwarz SMU200A Vector Signal Generator Operating Manual. Rohde & Schwarz 2012. Date of retrieval 12.9.2013. Available at: http://cdn.rohde-schwarz.com/dl_downloads/dl_common_library/dl_manuals/gb_1/s/smu200a_1/RS_SMU200A_Operating.pdf

31. Test-System Development Guide, Computer I/O Considerations. Agilent Technologies, Inc 2004. Date of retrieval 24.10.2013. Available at: http://cp.literature.agilent.com/litweb/pdf/5988-9818EN.pdf

32. Triquint 856831 duplexer datasheet. Triquint Semiconductor inc. 2011. Date of retrieval 1.3.2014. Available at: www.triquint.com/products/d/DOC-B-00000229

33. Using Service Requests in your GPIB application. National Instruments 2006. Date of retrieval 15.1.2014. Available at: http://www.ni.com/white-paper/4629/en/

34. White Paper, Quadrature Amplitude Modulation. National Instruments 2012. Date of retrieval 15.11.2013. Available at: http://www.ni.com/white-paper/3896/en/

35. Wilkerson, Jonathan R. 2010. Passive Intermodulation Distortion in Radio Frequency Communication Systems. Raleigh: North Carolina State University. Date of retrieval 20.9.2013. Available at: http://repository.lib.ncsu.edu/ir/bitstream/1840.16/6925/1/etd.pdf

APPENDICES

1. Appendix 1: Block diagram of network analyzer VI used in calibration
2. Appendix 2: MATLAB functions created for thesis

Block diagram of network analyzer VI used in calibration

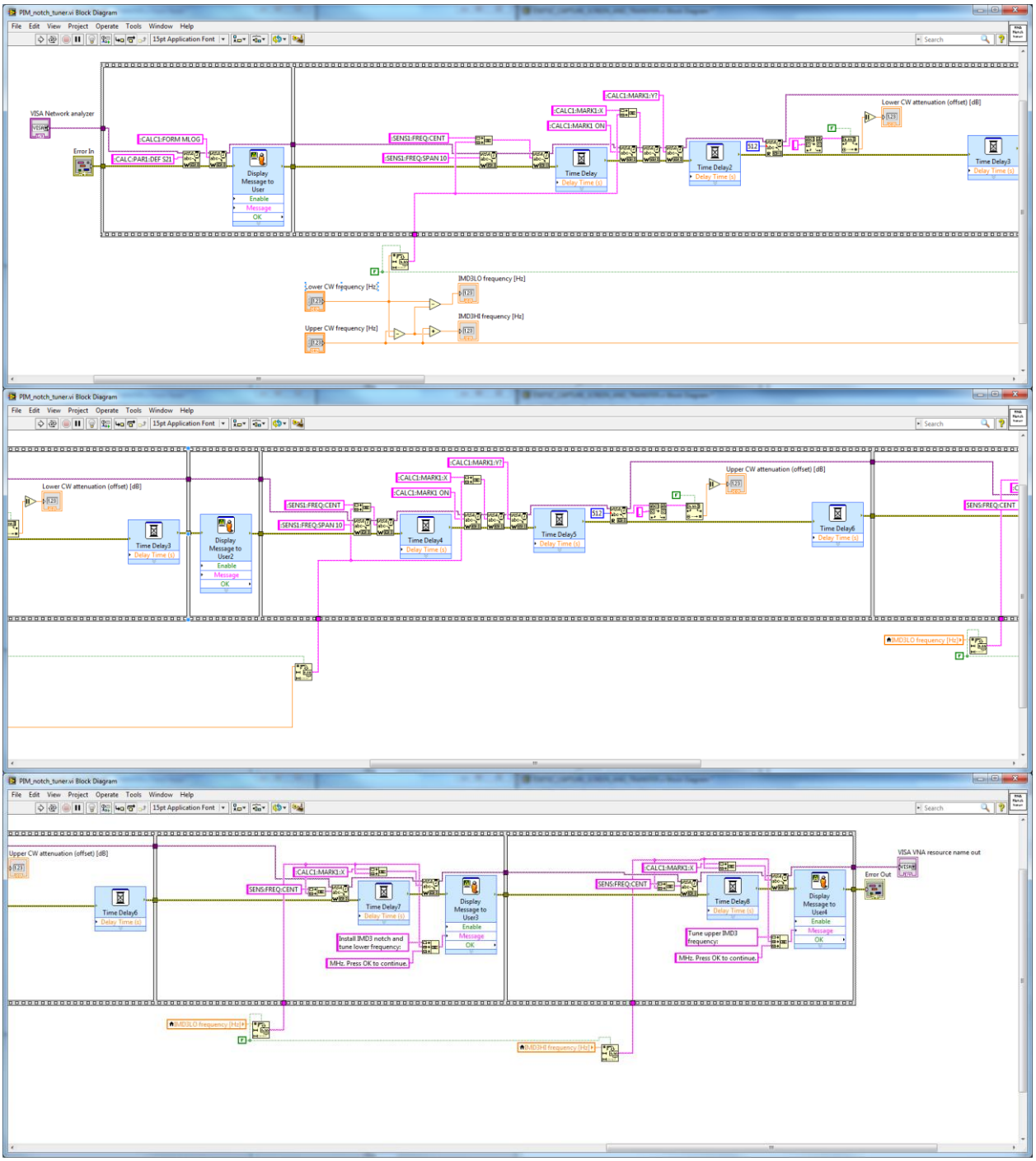

MATLAB functions created for thesis

```
function out = generateRandomSignal

x = complex(randn(30000,1),randn(30000,1)); %30000 samples of random
noise, complex spectrum

[b,a] = firls(600,[0 9.02/140 10/140 1],[1 1 0 0]); %FIR channel fil-
ter generation, 600 taps, passband 9.02/140

out = filter(b,a,x); %Apply generated channel filter to generated ran-
dom signal



function [out] = nonlinearModel(x)

A = 1;
B = -0.02;
C = -0.06;
D = -0.02;
out = A*x-B*x.^3+C*x.^5-D*x.^7;
```